Case Studies in Construction Materials 21 (2024) e03943

Contents lists available at ScienceDirect

Case Studies in Construction Materials

journal homepage: www.elsevier.com/locate/cscm

Raw materials and building technologies in the public buildings of Pompeii after the earthquake of 62/63 CE: A diachronic analysis of mortars

Matteo Maria Niccolò Franceschini [a,b], Giacomo Casa [a,b], Sara Calandra [c,d], Tommaso Ismaelli [a], Celestino Grifa [e], Mariano Mercurio [e], Valeria Amoretti [f], Gabriel Zuchtriegel [f], Emma Cantisani [a,*]

[a] CNR ISPC, Institute of Heritage Science, 10-via Madonna del Piano, Sesto Fiorentino, Florence 50019, Italy
[b] UNIROMA1, Department of Science of Antiquities, Sapienza University of Rome, 5-Piazzale Aldo Moro, Roma 00185, Italy
[c] UNIFI DICUS, Department of Chemistry "Ugo Schiff", University of Florence, 13-Via della Lastruccia, Sesto Fiorentino, Florence 50019, Italy
[d] UNIFI DST, Earth Science Department, University of Florence, 4-Via La Pira, Florence 50121, Italy
[e] UNISANNIO DST, Department of Science and Technology, University of Sannio, Via dei Mulini 59/A, Benevento 82100, Italy
[f] Archaeological Park of Pompeii, via Plinio, 26, Pompeii, Naples 80045, Italy

ARTICLE INFO

Keywords:
Mortars
Pompeii
Public buildings
Post-seismic restoration
Raw materials
Technologies

ABSTRACT

The paper deals with the technological aspects of the construction site of Pompeii through the characterization of the mortars, focusing on the identification of raw materials, their supply areas, selection criteria and mixing techniques to evaluate the continuity and changes in the different construction phases. Thanks to a multidisciplinary protocol that integrates archaeological, architectural, minero-petrographic and geochemical analyses, the study reveals that the binders were obtained from burning limestones from Mt. Lattari, while the aggregates are compatible with products from the Somma-Vesuvius volcano. The mortars from the period before 62/63 CE are characterised by a careful selection and preparation of the raw material, while the mortars from the period after 62/63 CE indicate a less precise procedures, probably due to the urgent need for reconstruction after the earthquake. Despite these changes, the essential quality and hydraulic properties of the mortars remained intact, demonstrating the resilience of ancient building practises.

1. Introduction

Ancient architectural restoration represents a practice that cities located in highly seismic areas necessarily had to deal with throughout their history. The multidisciplinary study of this phenomenon offers significant information to investigate ancient economy, society, and ideology but also allows scholars to reconstruct practical and theoretical knowledge of ancient architecture, which is only partially accessible through literary sources. Indeed, the analysis of the technical procedures discloses the local know-how of architects and craftsmen involved in the restoration of buildings and, could at the same time reveal technological improvements and the development of an earthquake-resistant building culture. Moreover, the study of restoration from a broader perspective allows us

* Corresponding author.
E-mail address: emma.cantisani@cnr.it (E. Cantisani).

https://doi.org/10.1016/j.cscm.2024.e03943
Received 10 September 2024; Received in revised form 29 October 2024; Accepted 1 November 2024
Available online 6 November 2024
2214-5095/© 2024 Published by Elsevier Ltd. This is an open access article under the CC BY-NC-ND license (http://creativecommons.org/licenses/by-nc-nd/4.0/).

to reconstruct the different approaches with which antiquity preserved its built heritage, as well as the socio-economic implications, ideological values and cultural meanings that lay behind this practical activity [1].

In this framework, Pompeii represents a highly significant context, as it was struck by a severe earthquake in 62/63 CE and the city was destroyed by the eruption of 79 CE. This provides the opportunity to study the historical phenomenon in a very precise time span. The aim of the research is to evaluate ancient architectural restoration, technological know-how and socio-economic dynamics of the community of Pompeii after the disaster.

As part of the historiographical debate on this topic, i.e. the final construction phase of Pompeii, earlier scholars have suggested that the city experienced a social and economic decline after 62/63 CE: according to a long-accepted interpretation, the Forum area was still in ruins at the time of the eruption, as a large open-air construction site that had not yet been restored to full functionality. This account of the Forum, first proposed by A. Mau and later by A. Maiuri [2–4], is deeply rooted in earlier studies and has been frequently revived [5–17]. However, in recent decades, this traditional assumption has been critically reviewed and challenged by more recent research, which showed that many public buildings were fully functional again after the earthquake. Moreover, the debate benefited from the introduction of new analytical methods and technologies, such as archaeoseismological and geophysical-geomorphological surveys [18–22].

Despite recent research providing a reassessment of the vitality of Pompeii during its last phase, all these studies have essentially focused on the study of masonry, i.e. construction techniques and stone and brick materials. However, in order to understand and evaluate the complexity of the restoration in its technological dimension, the contribution of other disciplines is required as part of an integrated and multidisciplinary protocol. In this respect, the study of mortars and binders through functional, petrographic, chemical and mineralogical characterization is crucial to gather important but overlooked information on the selection and preparation procedures of raw materials, as well as on the know-how and workflow on construction sites after 62/63 CE.

Concerning the methodology, many scholars used chemical, mineralogical, petrographic, and physical analyses of materials to acquire detailed information on the building's construction phases, changes of raw materials and production technologies of mortar-based materials in a diachronic perspective in archaeological and architectonic contexts [23–39]. As far as Pompeii is concerned, numerous data on Roman mortars and plasters have already been published [26,28,40–43], providing useful information on the mix design, the origin of the raw materials and the reconstruction of the construction phases, especially for private contexts (Table 1S).

1.1. Objectives

Our research aims to investigate the provenance of raw materials and technologies employed for the preparation of mortars in the various construction phases of the Pompeii Forum, integrating geochemical characterization of binders and aggregates of bedding mortars with morphometric and morphological properties of aggregates. Within the framework outlined above, the research has several objectives from an archaeological and analytical point of view. Previous studies have essentially focused on the search for confirmation/validation of chronologies previously proposed on an archaeological basis, through the grouping of samples and the search for correspondence between the stratigraphy of the masonry and the analytical data. However, this approach does not fully exploit the wealth of information that can be obtained from mortars.

In our perspective, tracing technical gestures and craft skills in the selection and processing of raw materials, as well as quality and technological standards, offers important insights into the history of ancient technology and architecture. In this respect, the aim of the research is to provide criteria and parameters to recognize traces of ancient gestures and to draw a picture of the history of craftsmanship in Pompeii. A specific focus was dedicated to the phases before and after 62/63 CE phases, in order to obtain detailed information on the technological changes in terms of mix design, type of raw materials and procurement strategies that occurred after the earthquake and, more generally, on the restoration dynamics and strategies adopted in the post-earthquake period, which represented a turning point in the biography of Pompeii.

1.2. Archaeological background

The analysis of the mortar required a preliminary examination of the surviving architectural evidence in order to identify the construction phases of the individual monuments prior to sampling. Thus, for the public monuments of the Forum, an in-depth study of previous research and a catalogue of stratigraphic units (SU) was carried out in order to assign each SU to a specific construction phase and to distinguish ancient restorations from modern repairs (Table 1). In distinguishing and classifying the SUs (stratigraphic units), the analysis takes into account the construction techniques (ashlar, *incertum, reticulatum, vittatum, vittatum* mixtum and brick masonry, see Table 2S), the materials used in the masonries (limestone, yellow and grey tuff, foam lava and black lava) and the information derived from the stylistic analysis of wall paintings (so-called Pompeian Styles) and architectural elements. The information obtained allows us to define three main chronological phases of the studied monuments on the Forum:

1) The first, dating back to the Samnite period (second half of the 2nd century BCE), includes the building projects of the Basilica, the Sanctuary of Apollo and the Temple of Jupiter.

2) A major phase of renovation dates back to the early imperial age (late 1st century BCE - early 1st century CE), when the eastern building (i.e., the Building of Eumachia, the so-called Sanctuary of the Public Lares and the Macellum), the southern civic offices, the so-called Comitium and the western honorary arch were built, while a travertine colonnade was erected along the western side of the Forum and in front of the Eumachia Building and of the so-called Sanctuary of the Public Lares.

3) Finally, an extensive restoration phase after the earthquake of 62/63 CE, includes the construction of the so-called Temple of *Genius Augusti* and of the eastern honorary arch and the reconstruction of many of the public buildings of the Forum. For each

Table 1
List of bedding mortar samples taken from public buildings in Pompeii and corresponding compressive strength estimated from penetrometric test.

ID sample	Building	Construction technique	USM	Description and conservation	Phase	Strength [MPa]
EU01A	Building of Eumachia	*Opus vittatum mixtum*	EU−9a	Façade on the Forum, northern rectangular exedra, north half of the eastern wall, lower sector, type B bricks and grey tuff small ashlar masonry, good state of preservation	Post−62/63 phase	4.6
EU01C	Building of Eumachia	*Opus vittatum mixtum*	EU−9a	Façade on the Forum, northern rectangular exedra, north half of the eastern wall, upper sector, type B bricks and grey tuff small ashlar masonry, good state of preservation	Post−62/63 phase	4.3
EU01D	Building of Eumachia	*Opus testaceum*	EU−5a	Façade on the Forum, northern rectangular exedra, east half of the northern wall, next to the NE corner, type A bricks masonry, good state of preservation	Early imperial phase	-
EU01E	Building of Eumachia	*Opus incertum*	EU−11b	Northern room behind the norther rectangular exedra, south half of the western wall, upper sector, lava and foam lava stones masonry, good state of preservation	Post−62/63 phase	-
EU02A	Building of Eumachia	*Opus incertum*	EU−40c	Inner court, northern rectangular exedra, western wall, upper sector, grey tuff, limestone and lava stones masonry, good state of preservation	Early imperial phase	4.0
EU02C	Building of Eumachia	*Opus incertum*	EU−40c	Inner court, northern rectangular exedra, western wall, lower sector, grey tuff, limestone and lava stones masonry, good state of preservation	Early imperial phase	-
EU03A	Building of Eumachia	*Opus incertum*	EU−58	Façade on the Forum, southern rectangular exedra, south half of the eastern wall, lower sector, limestone stones masonry, good state of preservation	Early imperial phase	4.6
EU03C	Building of Eumachia	*Opus testaceum*	EU−52	Façade on the Forum, southern niche, corner with the southern rectangular exedra, type B bricks masonry, good state of preservation	Post−62/63 phase	-
EU04A	Building of Eumachia	*Opus testaceum*	EU−209	North-east external corner, lower sector, type B bricks masonry, good state of preservation	Post−62/63 phase	4.5
EU04C	Building of Eumachia	*Opus incertum*	EU−205	Eastern external wall, plinth, between niches VI and VII, limestone and lava stones masonry, bad state of preservation	Modern phase	-
EU05	Building of Eumachia	*Opus vittatum simplex*	EU−192	Southern external wall, pillar between niches XV and XVI, grey tuff small ashlar masonry, bad state of preservation	Early imperial phase	-
GA06A	Temple of the *Genius Augusti*	*Opus testaceum*	GA−53a	Temple, northern external wall, lower sector, type B bricks masonry, good state of preservation	Post−62/63 phase	-
GA07A	Temple of the *Genius Augusti*	*Opus testaceum*	GA−2b	Vestibule, western wall, north half next to the entrance, lower sector, type B bricks masonry, good state of preservation	Post−62/63 phase	4.5
LPU09	Sanctuary of the Public Lares	*Opus testaceum*	LP−17b	Inner court, south side, eastern niche, eastern pillar, type C bricks masonry, bad state of preservation	Early imperial phase	4.3
LP10A	Sanctuary of the Public Lares	*Opus testaceum*	LP−36	Inner court, east apse, upper podium, southern pillar, lower sector, type C bricks masonry, good state of preservation	Early imperial phase	4.3
LP10C	Sanctuary of the Public Lares	*Opus testaceum*	LP−33	Inner court, east apse, lower podium, SO corner, type C bricks masonry, good state of preservation	Early imperial phase	4.3
LP11A	Sanctuary of the Public Lares	*Opus reticulatum*	LP−1a	Inner court, southern rectangular exedra, western external wall, next to the junction with the façade of the Temple of the *Genius Augusti*, grey tuff and foam lava stones masonry, good state of preservation	Early imperial phase	4.1
LP11C	Sanctuary of the Public Lares	*Opus testaceum*	LP−9	Inner court, south side, western niche, podium, type C bricks masonry, bad state of preservation	Early imperial phase	4.5
LP11D	Sanctuary of the Public Lares	*Opus reticulatum*	LP−1b	Inner court, southern rectangular exedra, west half of the southern wall, grey tuff and foam lava stones masonry, good state of preservation	Early imperial phase	4.5
MA12A	*Macellum*	*Opus testaceum*	MA−1	Façade on the Forum, western entrance, north passage, north pillar, type A bricks masonry, bad state of preservation	Early imperial phase	3.7
MA12C	*Macellum*	*Opus testaceum*	MA−90a	Inner court, north half of the western wall, next to the entrance, type A bricks masonry, bad state of preservation	Early imperial phase	-
MA13A	*Macellum*	*Opus reticulatum*	MA−21	Southern external wall, western half, lower sector, grey tuff stones masonry, good state of preservation	Post−62/63 phase	4.6
MA13B	*Macellum*	*Opus incertum*	MA−19	Southern external wall, western half, lower sector, lava stones masonry, good state of preservation	Post−62/63 phase	4.6
MA13C	*Macellum*	*Opus incertum*	MA−20	Southern external wall, western half, upper sector, limestone stones masonry, good state of preservation	Post−62/63 phase	-

(*continued on next page*)

Table 1 (*continued*)

ID sample	Building	Construction technique	USM	Description and conservation	Phase	Strength [MPa]
MA13D	*Macellum*	*Opus testaceum*	MA−23	Southern external wall, southern entrance, eastern pillar, lower sector, type D bricks masonry, good state of preservation	Post−62/63 phase	-
MA14A	*Macellum*	*Opus incertum*	MA−28c	Eastern external wall, northern half, lower sector, lava stones masonry, good state of preservation	Post−62/63 phase	4.6
MA14B	*Macellum*	*Opus incertum*	MA−28a	Eastern external wall, northern half, lower sector, lava stones masonry, good state of preservation	Post−62/63 phase	4.5
MA14C	*Macellum*	*Opus incertum*	MA−28a	Eastern external wall, northern half, lower sector, lava stones masonry, good state of preservation	Post−62/63 phase	4.4
MA14F	*Macellum*	*Opus incertum*	MA−29a	Eastern external wall, northern half, upper sector, limestone stones masonry, good state of preservation	Post−62/63 phase	-
TJ15A	Temple of Jupiter	*Opus incertum*	TG−1	Podium, eastern half of the northern side, lava stones masonry, good state of preservation	Samnite phase (II cent. BCE)	4.6
TJ15C	Temple of Jupiter	*Opus incertum*	TG−1	Podium, NE corner, lava stones masonry, good state of preservation	Samnite phase (II cent. BCE)	-
AG16A	Arch of Germanicus	*Opus testaceum*	AG−4	NE embedded pillar, north side, lower sector, type B bricks masonry, bad state of preservation	Post−62/63 phase	-
AG16B	Arch of Germanicus	*Opus testaceum*	AG−1b	Western side, SW corner, lower sector, brick masonry, good state of preservation	Post−62/63 phase	4.6
TA17A	Temple of Apollo	*Opus incertum*	AP−23	Inner court, west half of the northern wall, lower sector, grey tuff, limestone, lava and foam lava stones masonry, bad state of preservation	Post−62/63 phase	4.0
TA18A	Temple of Apollo	*Opus incertum*	AP−16	Inner court, southern half of the western wall, behind a plaster layer, limestone stones masonry, bad state of preservation	Early imperial phase	3.7
TA18B	Temple of Apollo	*Opus incertum*	AP−14	Southern external wall, western half, next to the southern entrance, limestone and lava stones masonry, bad state of preservation	Samnite phase (II cent. BCE)	-
TA19A	Temple of Apollo	*Opus incertum*	AP−82	Eastern pier wall, between pillars IV e V, lower sector, limestone ashlar masonry, bad state of preservation	Samnite phase (II cent. BCE)*	-
TA19C	Temple of Apollo	*Opus incertum*	AP−8a	Southern external wall, eastern half, limestone, lava and foam lava stones masonry, good state of preservation	Samnite phase (II cent. BCE)	-
BA20	Basilica	*Opus incertum*	BA−1	*Chalcidicum*, northern wall, lower sector, lava stones masonry, good state of preservation	Samnite phase (II cent. BCE)	4.5
DB21A	Building of *Duoviri*	*Opus testaceum*	ED−12	Eastern internal wall, norther half, next to the junction with the corner brick masonry, brick masonry, bad state of preservation	Post−62/63 phase	-
DB21B	Building of *Duoviri*	*Opus incertum*	ED−40	Western external wall, central part, lower sector, lava stones masonry, good state of preservation	Early imperial phase	-
TB22	*Tabularium*	*Opus testaceum*	TA−3c	Eastern internal wall, norther half, next to the podium of the norther niche, type B bricks masonry, good state of preservation	Post−62/63 phase	4.5
CU23A	Curia	*Opus testaceum*	CU−1b	Façade on the Forum, eastern half, next to the jamb of the passage between the Curia and the Building of Duoviri, type B bricks masonry, good state of preservation	Post−62/63 phase	4.4
CU23B	Curia	*Opus incertum*	CU−13b	Eastern external wall, central part, lower sector, grey tuff and limestone stones masonry, good state of preservation	Post−62/63 phase	-
CO24	*Comitium*	*Opus incertum*	CO−11	Inner court, norther wall, between pillar I and II, lower sector, grey and yellow tuff, limestone, lava and foam lava stones masonry, good state of preservation	Post−62/63 phase	-
FA25A	Temple of *Fortuna Augusta*	*Opus vittatum simplex*	FA−51	Cella, eastern wall, south of the apse, lower sector, yellow tuff small ashlar masonry, good state of preservation	Post−62/63 phase	4.2
FA25B**	Temple of *Fortuna Augusta*	*Opus incertum*	FA−51	Cella, eastern wall, south of the apse, lower sector, yellow tuff small ashlar masonry, good state of preservation	Post−62/63 phase*	4.8
FA25C	Temple of *Fortuna Augusta*	*Opus incertum*	FA−19b	Cella, eastern half of the norther wall, next to the eastern niche, limestone, grey tuff and foam lava stones masonry, good state of preservation	Early imperial phase	1.7
FA25E	Temple of *Fortuna Augusta*	*Opus testaceum*	FA−25	Cella, western wall, southern pillar of the entrance, lower sector, brick masonry, good state of preservation	Early imperial phase*	-
OD26A	*Odeion*	*Opus testaceum*	OD−1	Eastern entrance, southern jamb, lower sector, brick masonry, good state of preservation	Late-Republican phase	4.3
TH27A	Theater	*Opus testaceum*	TE−1	*Frons scaenae*, *valva regia*, western jambs, lower sector, type B bricks masonry, bad state of preservation	Post−62/63 phase	4.6
TH27B	Theater	*Opus testaceum*	TE−1	*Frons scaenae*, backwall, eastern half, between the apse and the rectangular exedra, lower sector, type B bricks masonry, good state of preservation	Post−62/63 phase	4.8

(*continued on next page*)

Table 1 (*continued*)

ID sample	Building	Construction technique	USM	Description and conservation	Phase	Strength [MPa]
TF28A	Triangular Forum	*Opus incertum*	FT−1	*Propylon*, western entrance, western jamb, yellow and grey tuff, limestone and lava stones masonry, good state of preservation	Post−62/63 phase	4.0
TI29A	Temple of Isis	*Opus incertum*	TI−1	Northern external wall, eastern half, lower sector, limestone, lava and foam lava stones masonry, good state of preservation	Post−62/63 phase	1.7

USM: masonry stratigraphic unit
* Uncertain construction phase
** lump samples unachievable

monument, the analysis allowed us to distinguish between the original SU and the various restorations carried out during the long history of the buildings, especially after the 62/63 CE earthquake.

2. Materials and methods

Following the archaeological investigation, mortar from different construction phases belonging to *incertum, reticulatum, vittatum mixtum* and brick masonries was extracted for each building (Fig. 1a-c).

To estimate the compressive strength of the bedding mortar in situ, a microinvasive test was carried out using a penetrometer (Fig. 1d). The test is based on measuring the penetration depth of a steel needle into a mortar joint that is repeatedly impacted with a known mass [44]. The device used is an RSM-DSC penetrometer with the following technical features: impact energy of 4.55 Nm, impact mass of 835 g and stroke of 82 mm. The result is determined by the needle penetration depth (mm) after 10 impacts using the correlation curve and the equation of the device [45]. The test served as a preliminary evaluation of the cohesive properties of the sample (Table 1).

The thin sections were examined with a polarised light microscope (PLM) using an AxioScope A1 Microscope at different magnifications, with video camera, 5 megapixel resolution and AxioVision image analysis software. The minero-petrographic examination of the mortars with the PLM makes it possible to identify the main aspects of the binders and detect the composition, the colour of the birefringence, the texture (micritic, microsparitic, sparitic recrystallizations), the microstructure (homogeneous, presence of patches, etc.), the interactions with the aggregate (e.g. reaction edges) and the presence of neoformation phases. As for the aggregates, PLM allows us to determine their composition, average grain size, grain size distribution and shape, as well as the binder/aggregate ratio and porosity.

To obtain detailed information on the selection and shape of the aggregates, ImageJ software was applied to the high-resolution photomicrographs of each sample [46,47]. This software allows the automatic determination of Feret diameter, the circularity ($C = 4\pi*A/(P^2)$, where A is the area of the particle and P is the perimeter of the particle) and the roundness ($R= 4*A/(\pi*(\text{major axis}^2))$). The Feret diameter was used to evaluate Φ, expressed as $\Phi = -\log_2$ (Feret min). These values allow the definition of the grain size distribution (GSD) of the aggregates for each sample [48].

The particle shape was described according to UNI 11176–2006 [49]. The roundness parameter quantifies the elongation of the particles. If the value for roundness is 1, the particle is a circle. The greater the elongation of the particle, the closer the roundness value is to 0. The circularity parameter is linked to the irregularity of the particle circumference. If the value for circularity is 1, the particle is a circle. The greater the irregularity of the circumference, the closer the value for circularity is to 0.

X-ray diffraction on powders (XRPD) was used to obtain a mineralogical bulk analysis of all samples and selected lumps. The latter were identified under a stereomicroscope. An X'Pert Pro PANalytical diffractometer equipped with an X Celerator detector with a Cu X-ray tube ($\lambda= 1.54$ Å) and using a Ni-filtered Cu Kα radiation source was used. The diffraction patterns were recorded under the following conditions: current intensity of 30 mA, voltage 40 kV, explored 2θ range 3–70°, step size 0.02° and total time per pattern of 16 min 27 s. The X'Pert HighScore program and the ICCD database were used for mineralogical phase identification.

The microstructural and semi-quantitative chemical analyses of the polished thin sections were performed using a SEM-EDS (ZEISS EVO MA 15) with W filament equipped with an energy dispersion EDS/SDD analysis system, Oxford Ultimax 40 (40 mm^2 with a resolution of 127 eV @5.9 keV) with Aztec 5.0 SP1 software. Binders, aggregates and lumps were analysed under the following conditions: acceleration potential of 15 kV, 500 pA beam current, working distance between 9 and 8.5 mm; 20 s live time as acquisition rate to archive at least 600,000 cts, according to Co standard, process time 4 for point analyses; 500 μs pixel dwell time to acquire maps with a resolution of 1024×768 pixels. The programme used for microanalysis was Aztec 5.0 SP1 software, which uses the XPP matrix correction scheme developed by Pouchou and Pichoir in 1991 [50]. Using the SEM-EDS data, for binders and lime lumps, the hydraulicity index HI [51] was calculated; the geochemical and microstructural analyses of minerals (clinopyroxenes and feldspars) and magmatic rock fragments were carried out for the aggregates.

Thermogravimetric analysis (TGA) is used to characterise binders (air binder, hydraulic binder, gypsum, etc.) in historical mortars. A Netzsch STA 449 F3 Jupiter thermal analyzer was used for thermogravimetric (TG) and differential scanning calorimetric (DSC) analyses. Data analysis was carried out using Netzsch Proteus 6.1.0 and Opus 7.0 software. The analysis was performed on powdered samples (approximately 30 mg, sieved at 0.063 mm) with a temperature range of 30–1000 °C and a heating rate of 10 °C/min. The most important parameters are the weight loss: in the temperature range of 200–600 °C, the dehydration of the aluminosilicates is

Table 2
Mineralogical composition (semiquantitative data) of Pompeii mortar samples.

ID sample	Cal	Qz	Pl	Kfs	Cpx	Feldspathoid		CASH, CAS	Gp	Ms
						Lct	Anl			
EU1A	+++	-	+	+	+	-	+	-	-	*
EU1C	++	-	+	+++	+	+	+	-	-	-
EU1D	++	++	++	+++	+	-	-	-	-	+
EU1E	+++	-	++	+	+	+	+	-	*	+
EU2A	+++	-	+	-	+	+	+	-	-	*
EU2C	+++	-	++	-	+	+	++	+	-	-
EU3A	+++	-	+	++	+	+	+	*	-	-
EU3C	+++	-	+	+	+	-	+	*	+	+
EU4A	++	-	-	++	++	+	+	-	-	-
EU4C	+++	-	+	+	+	-	+	-	-	+
EU5	+++	-	++	+	+	-	+	-	-	+
GA6A	++	-	+++	-	+	-	+	+	+	+
GA7A	+++	-	+	++	+	-	+	-	-	+
LP9	+++	-	++	-	-	-	+	-	*	+
LP10A	+++	+	+	+	+	-	*	-	-	*
LP10C	+++	+	+	+	+	-	+	*	-	*
LP11A	+++	-	++	++	++	-	+	-	+	+
LP11C	+++	-	++	++	+	-	+	-	-	*
LP11D	+++	-	+	+	+	-	+	*	-	*
MA12A	+++	-	+	+	+	-	+	-	-	+
MA12C	+++	+	-	-	-	-	-	+	-	-
MA13A	+++	-	+	+	+	-	+	-	-	*
MA13B	+++	-	+	-	-	-	+	-	-	-
MA13C	+++	-	+	+	+	-	+	-	-	-
MA13D	+++	-	+	++	++	-	+	-	-	-
MA14A	+++	-	+	+	+	-	+	-	-	-
MA14C	+++	-	++	++	+	-	+	-	-	-
MA14D	+++	-	+	+	+	-	+	-	-	-
MA14F	++	-	+++	+	+	-	+	-	*	-
TJ15A	++	-	++	++	+	-	++	-	-	-
TJ15C	+++	-	+	+	+	-	+	-	-	-
AG16A	+++	-	++	++	+	-	+	-	+	-
AG16B	+++	-	-	+	*	-	-	-	-	-
TA17A	+++	-	+	-	+	-	*	-	-	*
TA18A	+++	-	+	+	+	-	+	-	-	*
TA18B	+	-	++	+	+	-	+	+	+++	-
TA19A	++	-	+++	-	+	-	+	+	+	*
TA19C	++	-	+++	+	+	-	+	++	+	*
BA20	+++	-	++	++	+	-	+	-	-	-
DB21A	+++	-	+	+	-	-	+	+	+	-
DB21B	++	-	-	+	+	-	*	-	*	*
TB22	++	-	+++	++	+	-	+	++	-	-
CU23A	+++	-	++	-	+	-	+	-	-	*
CU23B	+++	-	+	-	+	+	-	-	+	-
CO24A	+++	-	++	+	+	-	*	-	-	*
FA25A	+++	-	+	+	+	+	-	-	*	-
FA25B	+++	+	-	*	-	-	-	-	-	*
FA25C	+++	+	+	+	+	-	*	-	-	-
FA25E	+++	-	-	+	+	*	-	-	-	-
OD26A	+++	+	+	-	+	-	*	-	-	*
TH27A	+++	-	-	+	+	*	-	-	-	-
TH27B	+++	-	+	+	+	-	+	-	-	-
TF28A	+++	+	-	+	+	*	+	-	-	*
TI29A	++	-	-	++	+++	*	-	-	-	*

+++: very abundant; ++: abundant; +: present; *: traces; -: below detection limit. Cal: calcite ($CaCO_3$), Qz: quartz (SiO_2), Pl: plagioclase ($NaAlSi_3O_8$-$CaAl_2Si_2O_8$, albite-anorthite series), Kfs: K feldspar ($KAlSi_3O_8$); Cpx: clinopyroxene ($Ca(Mg,Fe)Si_2O_6$), Lct: leucite ($KAlSi_2O_6$), Anl: analcime ($NaAlSi_2O_6{\cdot}(H_2O)$), CASH, CAS: calcium aluminate silicate hydrates crystalline phases, Gp: gypsum ($CaSO_4{\bullet}2\ H_2O$), Ms: mica, e.g. muscovite ($KAl_2(Si_3Al)O_{10}(OH,F)_2$)). Detection limit 4 %.

registered, which determines the presence of hydraulic components; and in the temperature range of 600–900 °C, a weight loss due to the decomposition of CO_2 is observed [52]. The typical air-lime mortar values have CO_2/H_2O about 13 % and CO_2 about 35 % [53]. In addition, the TGA results can be compared with the HI calculated from point microchemical analyses using SEM-EDS [54]. The combination of TGA and SEM results allows a more robust characterization of the hydraulic properties of the mortar.

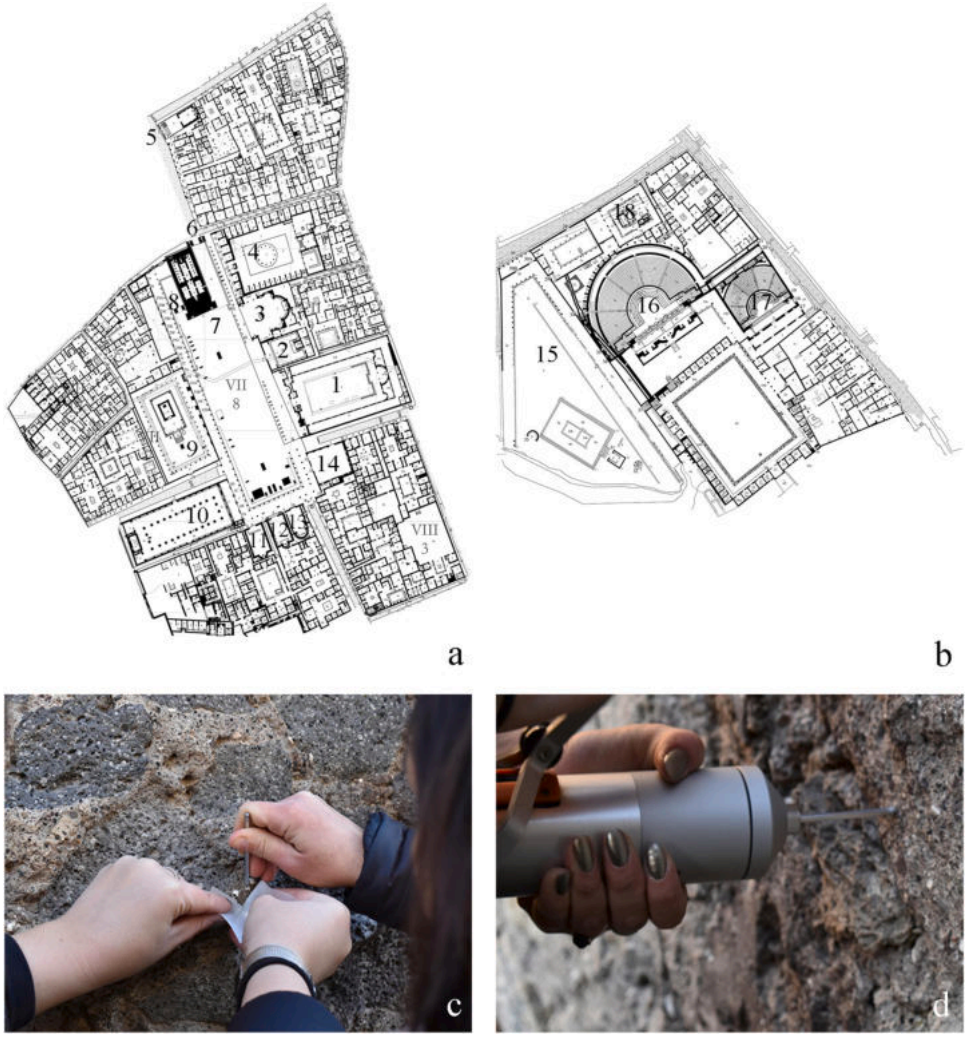

Fig. 1. Plan of the Civil Forum (a) and the Triangular Forum (b) of Pompeii with area of the bedding mortars sampling: 1) Building of Eumachia (EU); 2) Temple of the *Genius Augusti* (GA); 3) Sanctuary of Public Lares (LP); 4) *Macellum* (MA); 5) Temple of *Fortuna Augusta* (FA); 6) Arch of Germanicus (AG); 7) Temple of Jupiter (TJ); 8) Arch of Drusus; 9) Sanctuary of Apollo (TA); 10) Basilica (BA); 11) *Tabularium* (TB); 12) Curia (CU); 13) Building of *Duoviri* (DB); 14) *Comitium* (CO); 15) Triangular Forum (TF); 16) Theatre (TH); 17) *Odeion* (OD); 18) Temple of Isis (TI). Below, detail of the sampling phase (c) and penetrometric analysis *on site* (d).

3. Results and discussion

3.1. On site characterization

The mortar samples exhibit a pale brown to brown colour of the binder, with a scattered aggregate from medium to fine-grained sand, from fine to coarse-grained sand. In some samples, whitish and sometimes incoherent lumps of millimetres to centimetres were identified. Three penetrometric measurements (Table 1 shows the average) were taken at the sampling site. Only two samples have low strength values (1.7 MPa for FA25C and TI29A), while the others are between 3.7 and 4.8 MPa. These values demonstrate the good properties, high compactness and cohesion of the mortars, regardless of the construction techniques and the generally good state of preservation of the walls. The results of the penetrometric analysis agree with the reference data of pozzolanic mortars produced in the laboratory using different mix-design and taking into account old recipes [55–59].

3.2. Mineralogical and petrographic characterization

The most important mineralogical and petrographic features of the investigated mortars are summarised in Tables 2 and3S.

Table 3
Summary of the morphological results from the digital image analysis of the aggregates of selected samples.

Sample	Building	Constructive phase	Circularity	Roundness	Φmin	Φmax	Φmed	S(Φ)
EU1A	Building of Eumachia	Post−62/63	0.33	0.63	−2.40	3.82	2.31	0.93
EU1C	Building of Eumachia	Post−62/63	0.24	0.61	−1.81	5.88	2.86	1.14
EU1D	Building of Eumachia	Early imperial	0.25	0.57	−0.75	4.35	3.10	0.79
EU1E	Building of Eumachia	Post−62/63	0.36	0.60	−0.88	4.54	2.93	0.88
EU2A	Building of Eumachia	Early imperial	0.48	0.60	−1.04	4.92	3.23	0.81
EU2C	Building of Eumachia	Early imperial	0.49	0.62	−2.46	4.76	3.19	0.80
EU3A	Building of Eumachia	Early imperial	0.40	0.61	−1.28	4.38	3.03	0.81
EU3C	Building of Eumachia	Post−62/63	0.38	0.61	−1.20	4.76	3.00	0.93
EU4A	Building of Eumachia	Post−62/63	0.26	0.61	−2.85	4.97	3.02	0.91
EU4C	Building of Eumachia	Modern	0.25	0.60	−1.84	3.88	2.36	0.77
GA6A	Temple of the *Genius Augusti*	Post−62/63	0.28	0.61	−2.09	3.56	2.18	0.87
LP10C	Sanctuary of the Public Lares	Early imperial	0.50	0.62	−1.48	4.84	3.08	0.95
LP11A	Sanctuary of the Public Lares	Early imperial	0.55	0.66	0.07	3.52	2.21	0.79
LP11D	Sanctuary of the Public Lares	Early imperial	0.42	0.62	−0.80	4.29	2.89	0.93
MA12A	*Macellum*	Early imperial	0.52	0.65	0.18	4.32	2.79	0.90
MA13A	*Macellum*	Post−62/63	0.18	0.62	−1.02	4.68	2.98	0.83
MA13C	*Macellum*	Post−62/63	0.31	0.64	−1.68	3.54	2.34	0.86
MA14C	*Macellum*	Post−62/63	0.31	0.64	−2.24	4.61	2.94	0.90
MA14F	*Macellum*	Post−62/63	0.30	0.63	−1.90	4.44	2.97	0.91
TJ15A	Temple of Jupiter	Samnite	0.31	0.57	−0.72	4.54	3.11	0.76
TJ15C	Temple of Jupiter	Samnite	0.30	0.62	−1.43	3.52	2.49	0.74
TA17A	Temple of Apollo	Post−62/63	0.27	0.62	−1.03	4.54	3.04	0.79
TA18A	Temple of Apollo	Early imperial	0.32	0.59	−1.28	4.32	3.02	0.74
TA18B	Temple of Apollo	Samnite	0.29	0.61	−1.51	4.54	2.81	0.99
TA19C	Temple of Apollo	Samnite	0.34	0.61	−2.19	4.32	2.94	0.91
BA20a	Basilica	Samnite	0.36	0.61	−1.08	4.76	3.13	0.97
DB21A	Building of Duoviri	Post−62/63	0.17	0.60	−1.07	4.16	2.81	0.92
DB21B	Building of Duoviri	Early imperial	0.31	0.59	−1.87	4.38	2.90	0.94
TB22	*Tabularium*	Post−62/63	0.23	0.62	−1.37	4.32	2.79	0.98
CU23B	Curia	Post−62/63	0.21	0.58	−1.28	5.11	2.95	0.92
FA25A	Temple of *Fortuna Augus*ta	Post−62/63	0.29	0.62	−1.04	5.97	2.46	0.75
FA25C	Temple of *Fortuna Augusta*	Early imperial	0.48	0.65	−1.25	3.76	2.28	0.84
FA25E	Temple of *Fortuna Augusta*	Early imperial	0.44	0.60	−1.95	5.38	2.85	0.98
OD26A	*Odeion*	Late republican	0.33	0.61	−1.13	4.76	3.09	0.79
TH27A	Theater	Post−62/63	0.29	0.60	−2.07	4.72	3.08	0.80
TH27B	Theater	Post−62/63	0.25	0.60	−1.05	5.27	3.07	0.78
TF28A	Triangular Forum	Post−62/63	0.24	0.61	−0.19	4.64	3.03	0.78
TI29A	Temple of Isis	Post−62/63	0.29	0.64	−2.65	4.44	2.78	1.20

3.2.1. Mineralogical, textural, and chemical features of binders

Petrographic examination of the mortars reveals a heterogeneous binder characterised by different microtextures ranging from micritic to microsparitic up to sparitic (Fig. 2a-b). The presence of evident reaction rims between the binder and the volcanic aggregate indicates the formation of a natural hydraulic binder obtained by mixing air- lime with pozzolana as described in Vitruvius (5.12.2) and observed in recent studies [60–64] (Fig. 2c). The binder/aggregate ratio varies from 3/1 (sample FA25B) to 1/4 (sample EU1D), but most samples have a B/A ratio of 1/2 or 1/3.

PLM observation allows the identification and characterization of lumps, which are described as grains with a "whitish appearance, sometimes inconsistent" [52,65,66]. Their presence in lime-based mortars indicates that the lime was produced using a traditional technology in which the quicklime lumps are slaked with excess water to obtain a white paste (lime putty). The formation of lumps can be associated with: i) under- or over-burning of carbonate rock during the calcination process, ii) a lack of water during slaking and iii) inhomogeneous mixing of the binders with the aggregates [67,68]. The occurrence of lumps due to insufficiently calcined carbonate rock makes it possible to identify the type of carbonate rock that was calcined to produce the lime [60,67,69–71]. The presence of lumps in the binder of the Pompeian mortars is very common (Fig. 2c-d): millimetre-sized lumps have been observed, which can be attributed to firing residues with signs of residual features of the stone and remnants of unmixed binder. The presence of over-burned lumps, on the other hand, is very rare.

Porosity ranges from high to low, generally due to rounded pores and shrinkage cracks. However, the samples are generally compact and cohesive, confirming the observations of the on-site penetrometric analysis.

The TGA analyses were carried out on the enriched binder content of all mortars and on the lumps of some samples. Decisive parameters for distinguishing the type of mortar binder are the temperature ranges 200–600°C and 600–900°C and the corresponding weight loss. The decrease in mass between 200–600°C indicates dehydration of the aluminosilicate, also known as hydraulic water. The decrease in mass between 600–900°C results from the release of CO_2 due to the carbonation of calcium hydroxide (expressed as CO_2%). The weight loss due to carbonation and hydraulic water in all tested binder samples is typical for hydraulic mortars, especially for pozzolanic mortars [53]. Consistent with the construction phase, it can be observed that the values of hydraulic water are lower in the binder samples from the Samnite phase, ranging from 4.1 % to 7.2 %, compared to the early imperial (ranging from 4.8 % to 9.9 %)

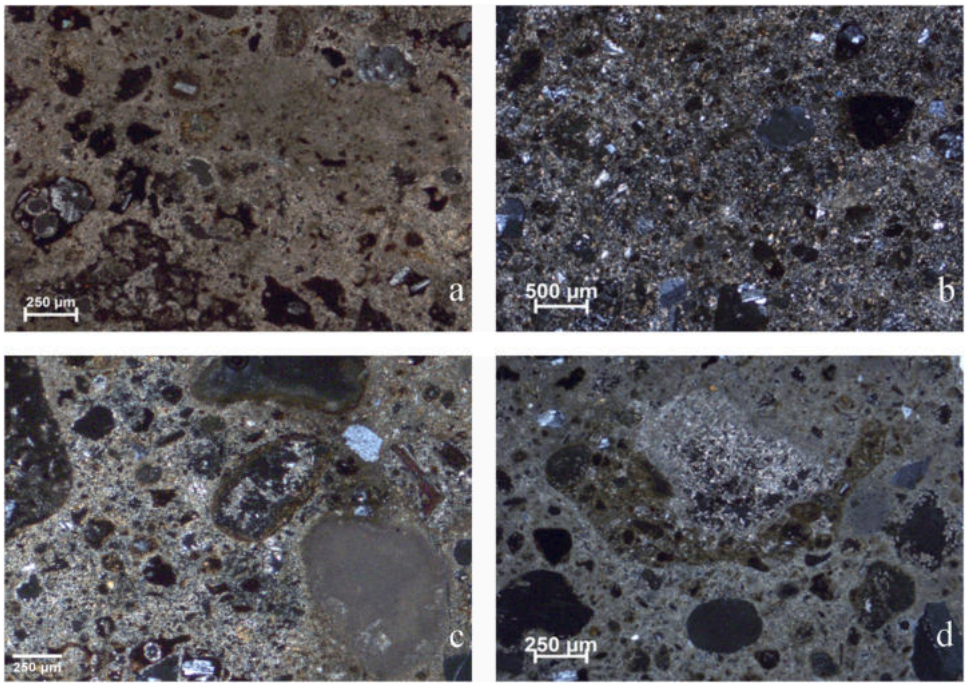

Fig. 2. Microphotographs of mortars (crossed nicols) and petrographic characteristics of the binder: a) micritic binder texture in sample EU2A; b) microsparitic binder texture in sample DB21A; c) lime lump and reaction rims between the binder and the volcanic aggregate in sample EU4A; d) heterogeneous lump with limestone remains in sample MA14F.

and Post-62/63 CE phase groups (ranging from 4.4 % to 9.0 %). The TGA results of these latter two phases are comparable and very similar, similar to the CO_2% ranges, for the early imperial samples between 13.5 % and 24.5 % and for the post-62/63 CE between 12.3 % and 22.2 %. The TGA analysis indicates a lower carbonate content and greater coherence for the Samnite period mortar samples (from 13.8 % to 16.9 %) than for the other two periods. However, the CO_2 content is still far below the theoretical value for an air lime binder, into which the tested mortars of the group fall.

The chemical composition of the binders and lumps in terms of the major elements, determined by SEM-EDS (Table4S), allowed us to evaluate the hydraulic behaviour using the HI-Boynton formula. The data confirm the results previously obtained using TGA (Fig. 3a-b). The HI values are in the range of 0.12–0.52 for the binder (from weakly to highly hydraulic mortars) and 0.01–0.10 for the lumps (air-hardening mortars, except for samples EU1C and BA20, which have higher values). On this basis, we can assume that the hydraulic mortar properties depend only on the chemical reaction between the binder and the pozzolanic aggregates and not on the type of binder. This consideration is confirmed by the thermogravimetric analysis of the lump, which falls into the air mortar cluster (Fig. 3a). These HI values, together with the petrographic observations and the SEM-EDS analysis, confirm that hydraulicity is closely related to the presence of finely dispersed pozzolanic material.

The constituents Si, Al and $Ca(OH)_2$ react to form calcium and aluminium hydrate silicates (C-A-S-H gel), phases that impart durability to the mortars, as evidenced below in the XRPD analysis.

In addition, the analysis of the lumps of the unburned residue allowed us to hypothesise the origin of the rock used for lime production. Both pure $CaCO_3$ lumps and lumps with a MgO content of up to 20 wt% were analysed (Fig. 4a-c), suggesting the use of limestones with Mg impurities (limestones and dolostones), possibly quarried in the Mt. Lattari [48,72].

In the same unburned lumps, areas with a higher MgO concentration (resulting from the decomposition of $CaMg(CO_3)_2$ into MgO) are observed. This concentration differs from that in areas consisting of almost pure $CaCO_3$ with residual crystallinity. This phenomenon is due to the difference in temperature of dissociation during calcination of Mg-rich carbonates, which starts at about 300°C [51,73,74], and Ca-rich carbonates, which occurs at ca. 850°C. This probably means that the temperature gradient in the kiln was evenly distributed and probably did not always reach 850°C. In addition, a variable MgO concentration of 1–4 wt% is observed in the binder, with subspherical dark nodules richer in MgO (> 10 wt%) and areas without MgO. This heterogeneity of the limestone can also be observed in the lumps of the same sample, some of which have the typical appearance of unmixed binder residues and others that of firing residues with Mg-rich nodules.

In the thin sections of the samples from the Sanctuary of the Public Lares, the Theatre, the Eumachia Building, the Temple of Apollo, and the *Tabularium* (i.e., EU2A, LP10A, LP11C, TB22, TH27A, TH27B), terrigenous zones are observed around the lumps (Fig. 4d). This suggests that limestone used as stone for lime probably was collected as available pebbles from detrital areas or stockpiles. The presence of not well preserved remains of bioclasts, as benthic foraminifera (Fig. 4b) and algae, strengthening the hypothesis about the origin of limestone used for the production of lime.

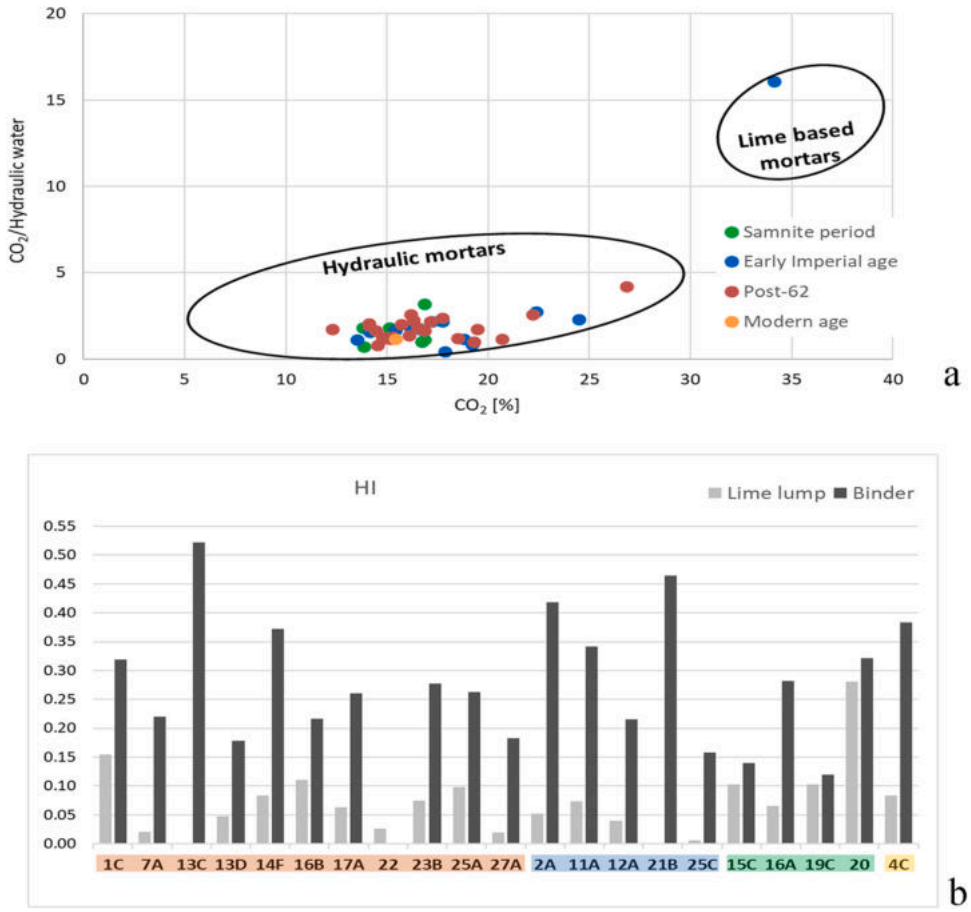

Fig. 3. Hydraulicity Index: a) HI obtained via TGA analysis of binder and lump; b) HI obtained by SEM-EDS using Boynton formula.

3.2.2. Mineralogical, textural, and chemical features of aggregates

The aggregate consists predominantly of igneous rock fragments with different textures (Fig. 5a-b-d-f), pyroclastic fragments (pumice and scoriae) (Fig. 5a-c-e) and single crystals (clinopyroxenes, plagioclase, leucite/analcime, and K-feldspars) (Fig. 5d-f). In addition, cocciopesto (crushed ceramics) with a maximum grain size of 1.4 mm and a sub-angular shape was identified in samples AG16A-B, TA17A,TA18B, DB21A-B, FA25B and CU23B (Fig. 6c). Carbonate rock fragments such as marbles, micritic limestones and dolostones were observed in some samples (i.e. EU1D, EU2A, MA13D, MA14F, BA20, CU23B, TH27A-B) with different shapes, from angular, as in sample EU1D (Fig. 5g), to well-rounded, as in sample MA14F (Fig. 5h), and variable grain size (from 0.2 mm to 2.7 mm).

Regarding the textural arrangement, unimodal, skewed, and seriate GSDs were identified by the image analyses (Tables 3 and 2S). Seriate GSD presents particles with sizes ranging from 0.05 mm and 11 mm and are predominantly angular (i.e. samples EU1A, EU1C, EU4A). In the unimodal GSD most of the clasts rarely reach 3 mm and range from fine to coarse sand sized grains (Φ mainly from 2 to 4). The predominant shape is sub-rounded (i.e. samples MA12A, LP10C, LP11A, LP11D). Skewed GSD presents clasts in the range $-1<\Phi< 0$ and $2<\Phi< 3$. Their size is less than 3.5 mm. The grains can have heterogeneous shapes, ranging from sub-rounded to angular (i.e. samples BA20, TJ15C). The measured average roundness of each sample varies between 0.57 and 0.65, which means that the particles have the same elongation on average. The circularity, on the other hand, varies between 0.17 and 0.55. This difference may be largely due to the irregularity of the particle perimeters, and the lower C values indicate less round and increasingly angular aggregates.

Interestingly, sample TA17A (post-62/63 repair) contains a reused mortar fragment (Fig. 6a). It has a size of about 3 mm and was recognised due to its higher porosity, straight boundaries and a different colour and microstructure than the surrounding binder of the sample.

Volcanic rock fragments are the most common type of aggregate showing different textures: hyaline, cryptocrystalline, microcrystalline, and rare ophitic lavas.

The fragments of ophitic lavas are generally small, with a maximum size of 2 mm in sample MA13D (Fig. 5b); some of these fragments are in samples LP10C, MA13C-D, BA20, CU23A-B. The other lava types are extremely variable in size, ranging from very fine <0.05 mm to millimetre-sized fragments. Sample EU1A contains the largest hyaline fragment with a size of about 9 mm, and sample EU4A contains the microcrystalline lava fragment with an observed maximum size of 11 mm.

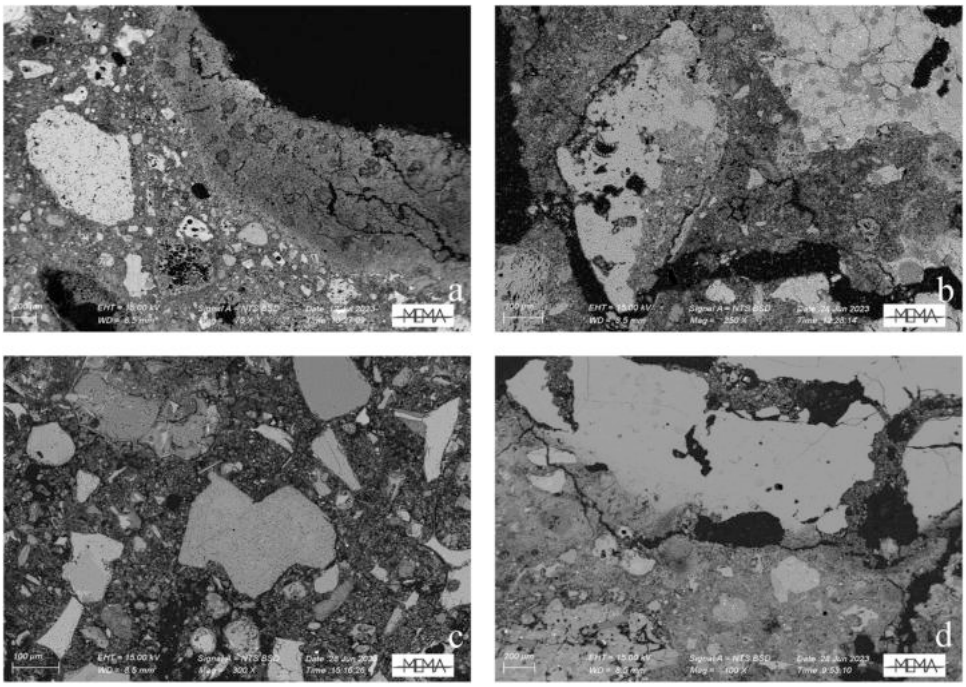

Fig. 4. Backscattered SEM image of lumps and carbonate fragments: a) heterogeneous lump texture with Mg inclusions in sample EU2A; b) the unburned lump of sample BA20 consisting of one part rich in Mg and the other exclusively of Ca (in this area a bioclast remnant is evident); c) subspherical dark nodules richer in Mg in sample TA17A; d) lime lump with terrigenous zones in sample TB22.

The shape of the lava fragments is generally angular, but there are also samples with strongly rounded fragments as in MA12A, EU2A, EU2C, EU1E, LP9, LP10A, LP10C, LP11A, LP11C, LP11D, FA25C, FA25E, which were probably rounded by erosion and transport processes.

Plagioclases, clinopyroxene, K-feldspar, and single crystals or as glomerophyre clasts of leucite/analcime (Fig. 6e-f) are the typical paragenesis of the magmatic rock fragments (i.e. EU1A, EU1C, EU1D, EU3C, EU4A, EU4C, MA13C, MA13D, MA14A-C, TJ15C, BA20, FA25C, FA25E, OD26). Some of these rock fragments also contain olivine crystals (rarely with iddingsite alteration phase).

All the above minerals can also be found as loose crystals with angular shape and millimetric size; especially, the clinopyroxene crystals can reach a size of 4 mm, such as in sample BA20. Samples EU2A and TJ15C also contain millimetre-sized clinopyroxene crystals with euhedral or pseudo-euhedral habits, often twinned, as well as very fine shards. This mixture of aggregates was probably formed by the grinding of lavas or scoriae.

LP 9, MA14A, CU23A samples contain garnet. Biotite is fairly abundant in samples DB21A, DB21B and LP10A.

Lavas, pumices, and volcanic scoriae are common pyroclastic products that were used as aggregates in Pompeian mortars.

Pumices are frequent (in samples EU1A, EU1C, EU3C, GA6A, GA7A, LP10C, LP11C, MA12A, TA18A, DB21A-B, TB22, CU23A, FA25B, FA25E), they are extremely porous, often with flamed textures (elongated and iso-oriented vacuoles) (Fig. 6d) and almost aphyric (in samples LP11A, LP11C, MA12A, TA18A). The well-rounded shape is very common for this type of aggregate with a maximum size of 5 mm (in samples EU1C and GA6A). Interestingly, sample MA12A contains a pumice that incorporates a single tiny carbonate fragment (Fig. 6b); this is probably a xenocryst eroded during the magma ascent.

Scoriae are also abundant; their vacuoles can sometimes contain crystals up to millimetres in size, and their pores can be very large and rounded (i.e., EU2C, EU3A, EU5, LP10A, LP11A, LP11D, MA12A, TJ15A, AG16A, TA17A, TA18A, FA25C, FA25E, TF28A, TI29A). Normally, the scoriae have a very angular shape probably due to their fragile and porous nature which makes them easily disintegrate into irregular fragments. Only in some cases, scoriae with a rounded shape are observed, as in EU2C and TI29A. The maximum scoriae size is nearly 9 mm in sample EU5, but in many samples scoriae slightly larger than one millimetre are found.

Rare pyroclastic products are seen in samples EU4C and AG16A, with sub-rounded shape and millimetric size. They have a glassy outer edge and an inner microcrystallinity with strong vacuolarity and tiny pores.

The chemical data obtained by SEM-EDS analysis on aggregate grains are listed in Table 5S. The silica content ranges from 52 to 56 wt%, and the alkali content ($Na_2O+ K_2O$) ranges from 7 to 11 wt% of lava fragments with compositions ranging from phono-tephrites to tephri-phonolites and from trachy-basalt to trachy-andesites in the TAS plot [75] (Fig. 7). Pyroclastic pumice and scoriae have SiO_2 content of 55–65 wt% and alkali content 12–15 wt%, showing phonolitic or trachytic compositions. As can be seen from Fig. 7, the mortars from the Samnite period do not contain any pumice stones and scoriae with phonolitic composition; in contrast, phonolites are very common in the other mortar groups.

The chemical data of the clinopyroxenes plotted in the corresponding ternary composition diagram (Fig. 8b) show that the

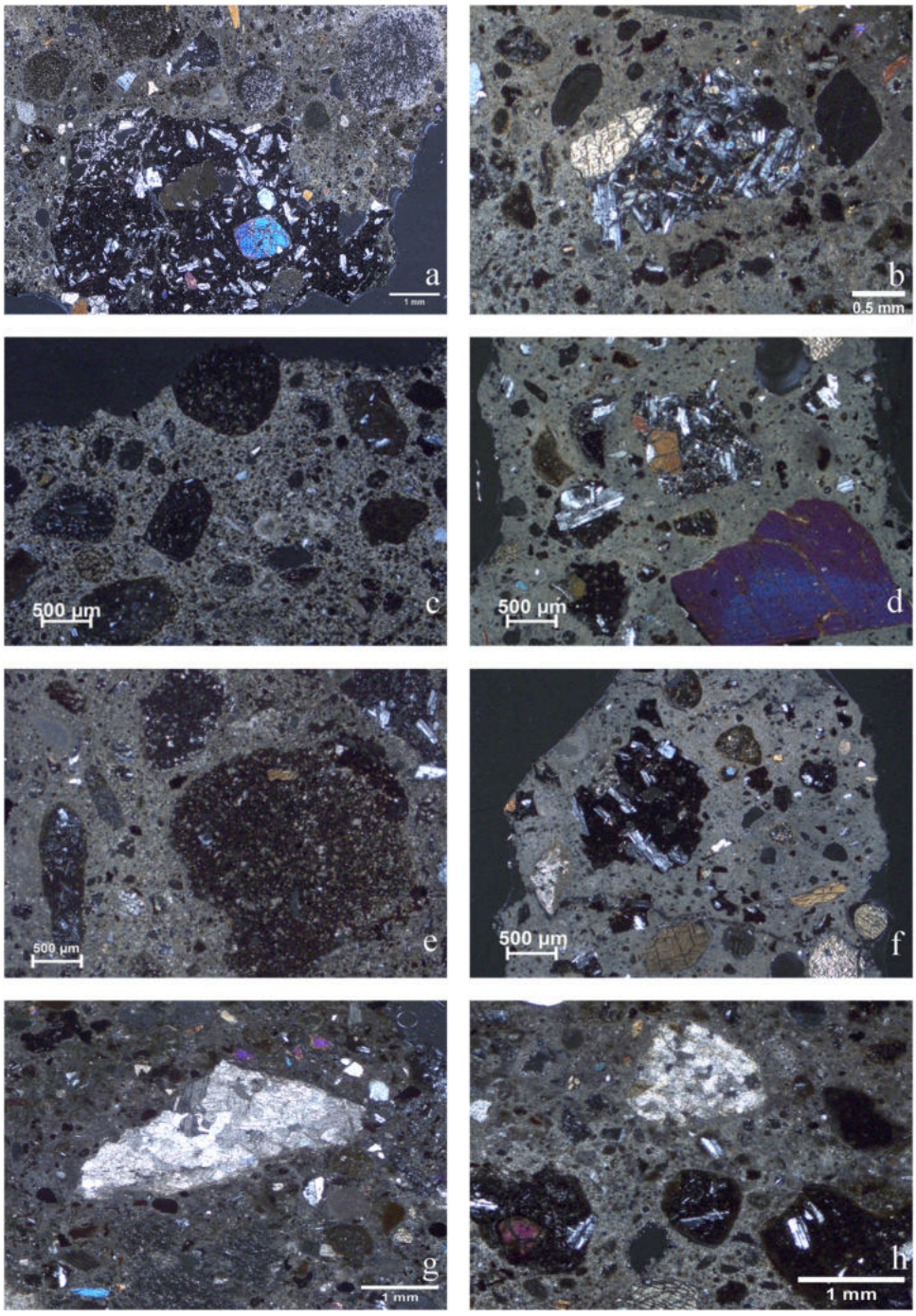

Fig. 5. Microphotographs of mortars (crossed nicols) and petrographic characteristics of the aggregates: a) cryptocrystalline lavas with pumices in sample EU1A; b) holocrystalline fragments in sample MA13D; c) scoriae composing subrounded aggregates in sample LP11A; d) microcrystalline lavas fragments and crystals of clinopyroxene and plagioclase composing angular aggregates in sample EU4A; e) scoriae and pumices in sample EU1A; f) hyaline lavas with crystals and a limestone fragment in sample BA20; g) marble fragment in sample EU1D; h) dolomite fragment in sample MA14F.

clinopyroxenes range from diopside ($CaMgSi_2O_6$) to hedembergite ($CaFeSi_2O_6$) with some Ca-rich crystals [76]. The ternary composition diagram of feldspars shows that plagioclases are mainly bytownites ((Ca0.7–0.9, Na0.3–0.1) [Al(Al,Si)Si_2O_8]) (with composition of anorthite between 90 and 70 and albite 10–30), while K-feldspars are sanidines ($K(AlSi_3O_8)$) [77] (Fig. 8a). All these data are compatible with the composition of the Somma Vesuvius products [78–81].

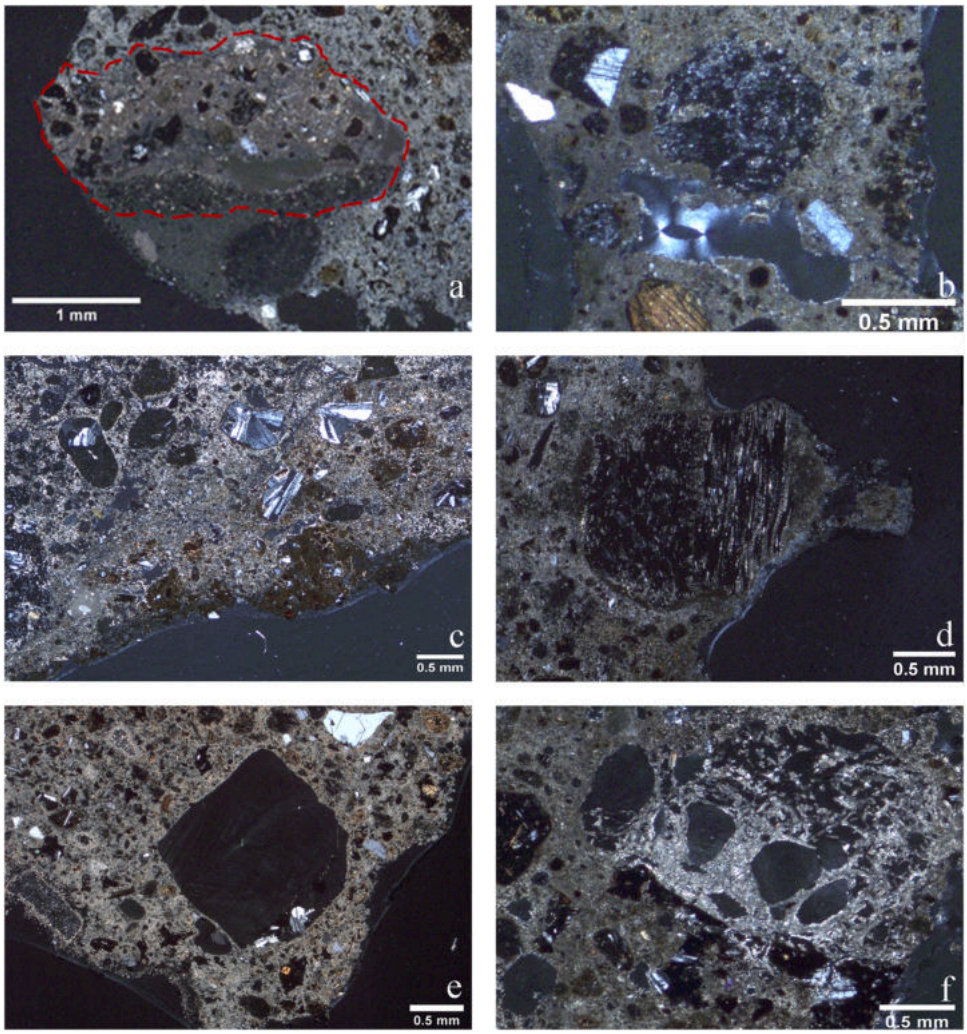

Fig. 6. Microphotographs of mortars (crossed nicols). Aggregate: a) reused mortar fragment in sample TA17A; b) pumice with carbonate rock inclusion in sample MA12A; c) cocciopesto fragments in sample DB12A; d) pumices with flamed texture in sample TA18A; e) single crystal of leucite in sample EU4C; f) glomerophyre of leucite in sample MA13C.

All mineralogical data, such as the leucite/analcime phenocrysts in the lava fragments, confirm that the aggregates of the Samnite Period samples are compatible with the Somma Vesuvius volcanic products, although juvenile rocks with trachytic composition are not common in the composition of the Somma Vesuvius magma [82], but are probably influenced by alteration processes and alkali leaching.

The TAS of the mortar aggregates from the early imperial period and the post-62/63 CE restoration fit the data on the composition of the volcanism originating from Somma Vesuvius [81,83]. This origin is confirmed by the presence of leucite and the rare garnet, as well as by the composition of clinopyroxenes and feldspars contained in the volcanics. In the mortars from the period after 62/63 CE the lava fragments show a greater variation in silica (67–49.9 wt%) and alkali (16.1–5.9 wt%) content.

A special case is sample EU4C, where the chemical composition of the lavas is more undersaturated in SiO_2 (48 wt%) with an high alkali content (10 wt%), suggesting a composition compatible with the magmatic products of Somma Vesuvius after 79 AD. This is also confirmed by euhedral millimetric leucite crystals observed in the thin sections and, consequently EU4C sample can be recognised as a modern restoration [27,43].

3.3. Mineralogy by XRPD

XRPD confirmed that most of the mortar samples present calcite as the main mineral phase. Clinopyroxenes, plagioclase, analcime and K-feldspars are the other identified volcanic phases, whose relative abundance varies in the samples. Quartz is an accessory mineral present in samples LP10A, LP10C, MA12C, FA25B-C, OD26A and TF28A (Table 2), while it is very abundant in sample EU1D. It is worth noting that most of the samples containing quartz are from the pre-62/63 CE phase, with the exception of FA25B and TF28A.

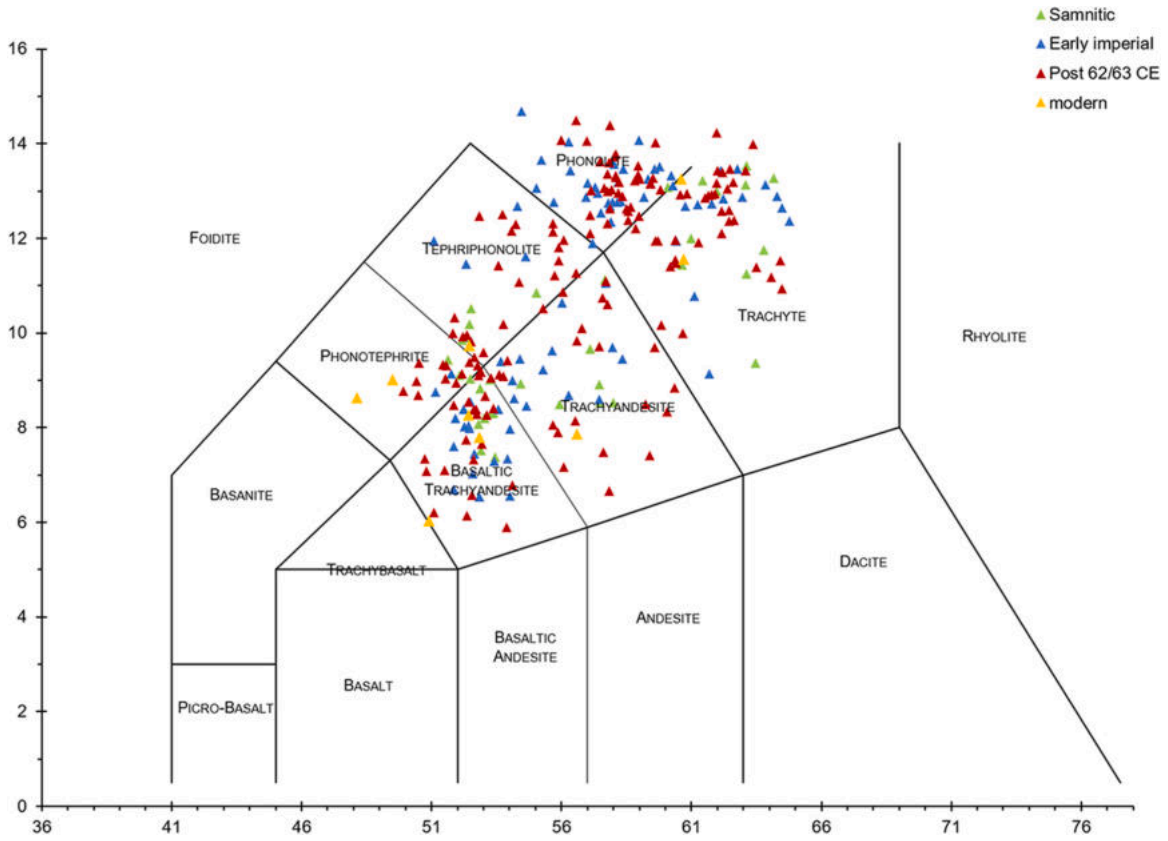

Fig. 7. Classification of mortars volcanic aggregates via TAS diagram.

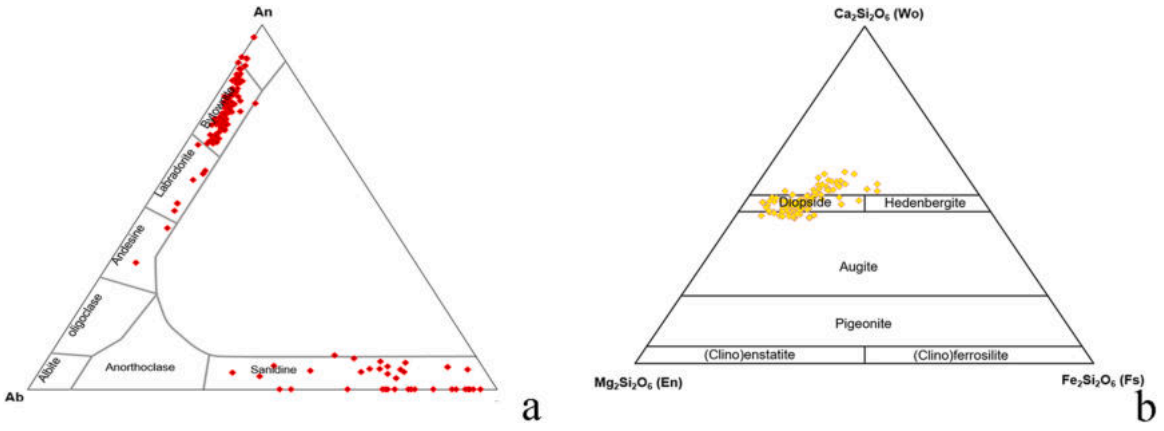

Fig. 8. Compositional diagrams of minerals: a) feldspars classification; b) clinopyroxenes classification.

Analcime, a product of leucite alteration [84], appears in all samples except EU1D, MA12C, AG16B, CU23B, FA25A, FA25B, FA25E, TH27A, TI29A. In contrast, the samples in which leucite was detected are relatively rare (samples EU1C, EU1E, EU2A, EU2C, EU3A, EU4A, CU23B, FA25A, FA25E, TH27A, TF28A, TI29A).

In sample TA18B, the abundant gypsum could be due to a carbonate sulfation process, but in several other samples it is present at least in trace amounts (EU1E, EU3C, GA6A, LP9, LP11A, MA14F, AG16A, TA19A, TA19C, DB21A-B, CU23B, FA25A) [85,86].

Finally, the XRPD analyses of samples TA19C, TB22, EU2C, EU3A, EU3C, GA6A, LP10C, LP11D, MA12C, TA18B, TA19A, DB21A show the presence of C-A-S-H phases (Fig. 1S), which are responsible for the hydraulicity of the mortars.

4. Implications

This minero-petrographic and geochemical characterisation of mortar samples from several public buildings in Pompeii allowed us to provide important insights into the supply chain of raw materials, as well as building technologies across several historical periods.

As far as the origin of the raw materials is concerned, there is considerable continuity between the 2nd century BCE and the post 62/63 CE period. In particular, the choice of stones from the Lattari Mountains seems to be confirmed for the production of lime, considering their accessibility and the use of Mg-lime or dolostones, as well as the presence of bioclasts. The choice of pozzolanic aggregates, which determine the degree of hydraulicity of the mortars due to the reactions between the aggregates and the binder, also shows continuity between the pre- and post-seismic phases. Only the 2nd century BCE samples are slightly less hydraulic than those from the Imperial period. In the case of the aggregates, the supply area can be identified on the basis of the textural and geochemical parameters in the products of Somma Vesuvius (Fig. 9).

Despite the continuity of supplying strategy, a clear variability in the processing of raw materials has been observed in the three main construction phases:

-mortars from the Samnite period (2nd century BCE) show a micritic binder, with a variable amount of lumps (unmixed binder and underburned fragments), heterogeneously shaped aggregates (circularity about 0.30), skewed GSD, rare pluri-millimetric clasts (maximum size around 3.5 mm), and a B/A ratio of 1/1–1/2. Some of the Samnite mortars present grinded scoriae and lava, to obtain a finer aggregate (TJ15A-C, BA20) (Fig. 10). From a technological point of view, the smaller size of the aggregates indicates selection procedures (possibly by sieving), while the fine-angular portion could indicate the grinding of scoriae and lavas. The presence of lumps of different origin indicates a lack of care both in the phase of cooking the limestone and in the phase of mixing the lime.

-mortars dated to the early imperial age (pre 62/63 CE) generally have micritic binder, with rare lumps, mainly unmixed binder, sub-rounded and well-selected aggregate (circularity ranging from 0.40 to 0.55) and a unimodal GSD with rare millimetric aggregates (usually maximum size ca. 3 mm). Almost all the samples have a B/A ratio of 1/2 (Fig. 11). From a technological point of view, the aggregate appears to have been selected for its reduced size, while the sub-rounded shape may indicate the targeted use of naturally selected aggregates, such as sands (river or coastal ones). Although rare, the predominant presence of binder remnants indicates a lack of care during the lime mixing phase. It is noteworthy that quartz was mainly observed in the early imperial samples. This mineralogical phase is the most over-saturated in silica, while all volcanoes in the Campania region are more or less under-saturated in silica. This suggests that the quartz in the Pompeian area is due to debris that was transported by rivers from the Apennines [27].

-mortars from walls built after 62/63 CE typically have a micritic to microsparitic binder, with abundant lumps (prevalently underburned fragments), angular aggregate (circularity < 0.31), and a seriate GSD with widespread millimetric clasts (maximum size about 11 mm). These samples have a B/A ratio tending towards 1/3. All these samples contain a rather coarse aggregate, with a greater textural variability and compositional, coupled with occasional reuse of mortar. The magmatic aggregate has a larger variation of silica

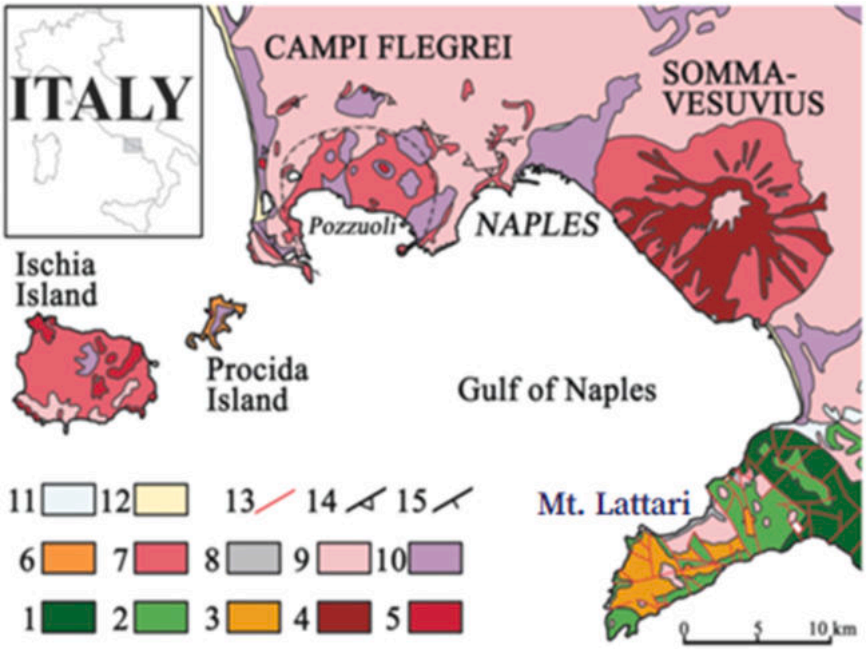

Fig. 9. Geological map of the bay of Naples: 1) Lower Cretaceous-Liassic carbonate platform deposits; 2) Upper Cretaceous rudistic limestones; 3) Serravallian-Upper Langhian pre- to late orogenic silicoclastic and carbonatic deposits; 4) ultrapotassic lavas (leucitic-basanite and leucititic series); 5) potassic lavas (shoshonitic series); 6) hyalotuffs; 7) pyroclastic flows and surges; 8) Campanian Ignimbrite pyroclastic deposits; 9) pyroclastic fall deposits; 10) volcano-sedimentary deposits; 11) Upper Pleistocene talus breccias; 12) Holocene beach and coastal dunes; 13) faults; 14) boundary of the CI caldera; 15) boundary of the NYT caldera. (modified after V. Morra et al. [80]).

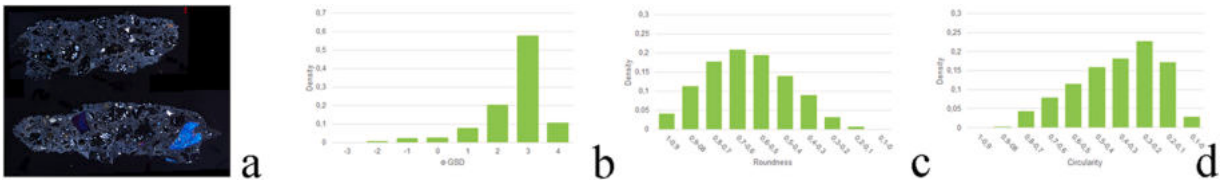

Fig. 10. Morphometric and morphological parameters of the Samnite phase: a) microphotograph of sample BA20; b) GSD; c) roundness; d) circularity.

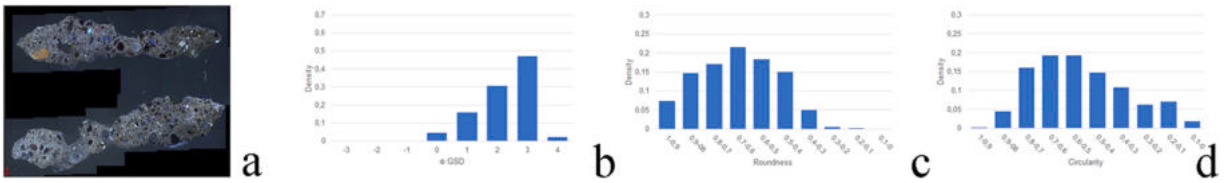

Fig. 11. Morphometric and morphological parameters of the early imperial phase:a) microphotograph of sample MA12A; b) GSD; c) roundness; d) circularity.

(67–49.9 wt%) and alkali (16.1–5.9 %) content (Fig. 12). From a technological point of view, the less attention in the choice of aggregate determined a greater variability in size and shape, texture and composition, and a greater presence of aggregate. The lower presence of lime may indicate the intent of saving materials, while maintaining good characteristics of the mortar. Finally, the abundant presence of traces of unburnt stones suggests a lack of attention during the burning phase, probably related to the uneven distribution of heat in the kiln or to the use of pieces of stone of different size.

The method based on the morphometric and morphological analysis of the samples proved successful in recognising two outliers, both taken in the Eumachia building, from masonries of the early imperial period (first decades of the 1st century CE): samples EU1D and EU4C. While all early imperial mortars of this building, in addition to the common features of pre 62/63 CE samples, have shards and glassy-edged crystals, perhaps due to the grinding of scoriae and lavas, both outliers had no such secondary characteristics. Sample EU1D shows a B/A ratio 1/4, the grains appear very angular with carbonate fragments (both marble and micritic limestone) as well as aggregates of sedimentary origin. These peculiar characteristics suggest that EU1D was a plaster, not a bedding mortar. As for sample EU4C, the presence of angular aggregates, including heavily under-saturated in silica lava glass (a characteristic of post-79 CE eruptions), as well as large leucites, possibly related to the 1631 CE eruption, indicate that it belongs to a modern restoration.

5. Conclusions

The result of the multi-analytical protocol allows us to follow the evolution of mortar technology across the different periods. The mortars of the Samnite phase exhibit a micritic binder with variable lumps and a heterogeneously shaped aggregate, suggesting a degree of selection and possibly the use of sieved or grounded scoriae and lava, as is assumed in the Basilica and the Temple of Jupiter, on the basis of the angular, finer portion of the aggregate.

The early imperial mortars are characterised by a careful selection and treatment of materials, with sub-rounded, well-selected aggregates and a uniform B/A ratio of 1/2. During this period, a deliberate use of naturally selected aggregates in certain natural basins, such as river or coastal sands, can be assumed. The almost exclusive presence of quartz in these samples could confirm this hypothesis, as this mineral phase is closely associated with the transport of fluvial debris in the area studied.

The processing of post-62/63 CE mortars exhibits a clear technological change. They are characterised by a micritic to microsparitic binder with abundant underburned lumps and coarser and angular aggregates, which appear to be not selected, as the seriate distribution shows. The B/A ratio tends towards 1/3, with greater textural variability and the occasional reuse of mortar, suggesting less strict selection procedures. These changes seem to indicate that less attention was paid in the meticulous preparation of the mortars, which was observed in earlier periods, forgoing the choice of aggregates, and reducing the amount of binder. Despite these variations,

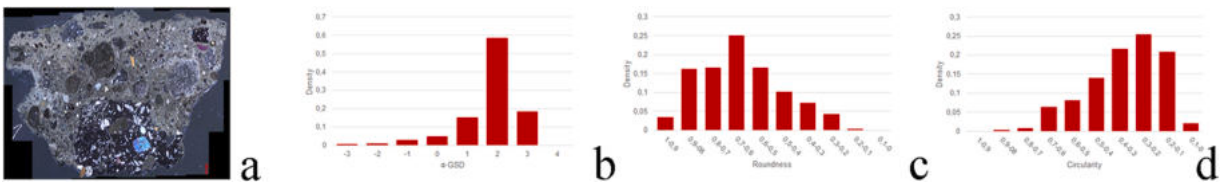

Fig. 12. Morphometric and morphological parameters of the post-62/63 CE phase: a) microphotograph of sample EU1A; b) GSD; c) roundness; d) circularity.

both the penetrometer data and the hydraulicity values do not indicate a general deterioration in the quality of the mortar, but only a few less cohesive samples. In fact, the hydraulic properties and cohesion of the mortars after 62/63 CE are still effective, suggesting that the reduction of care in the preparation phase has not significantly affected the structural integrity of the constructions and that the essential qualities required for the durability of the walls have been maintained.

These differences between the pre- and post-62/63 CE phases seem to reflect the urgent need for a rapid reconstruction after the earthquake, which led to an acceleration of the construction process, with a shortening in the execution time. This trend is comparable to other procedures already identified, all of which aim to speed up the reconstruction programme:

i. the optimisation of delivery times through the change of sources and supply chains and the massive import from the Phlegraean area of stocks of bricks and yellow tuff, materials specifically extracted and transported for the reconstruction of the city [87–90];
ii. the standardisation in production and construction of certain building materials, for example a new type of bricks, whose production seems specifically dedicated to the post-seismic emergency and whose on-site workmanship reveals standardised procedures [22,89,91];
iii. the reuse of materials recovered from collapsed structures, a practice probably extended to the marble slabs, architectural elements [92] and building materials, which were re-used in the wall facings as *scapoli* and in the wall cores as *caementa* [4,90, 93].

Nevertheless, from a qualitative point of view, the execution of the post-62/63 CE structures does not reveal any decline in quality, and therefore, within a discourse of substantial continuity of building techniques, it should be highlighted that the most sophisticated procedures, inherited from the late republican tradition, but not strictly necessary for the strength of the walls, were deliberately overlooked.

In conclusion, this paper contributes to the study of the evolution of Pompeian mortars over time, focusing on the period before and after 62/63 CE. The mortar samples were subjected to a well-established analytical protocol, that enabled their mineralogical, petrographic, and, in selected cases, chemical characterization. In addition to these analyses, a detailed digital image analysis of highly magnified microphotographs of the thin sections of the samples was carried out. The study of lumps and binders (texture, binder/aggregate ratio), as well as the morphometric and morphological features of the aggregate grains (Grain Size Distribution, Circularity, Roundness) highlighted by DIA, enabled the categorization of the samples based on common characteristics. Thanks to the solid chronological grid derived from the archaeological-architectural study, clustering demonstrated that mortars from the same period have similar characteristics.

This made it possible to reconstruct the evolution of Pompeian mortars, both in terms of technical gestures and the choice of raw materials. Furthermore, this study introduces a new set of criteria and protocols that can provide valuable data for the study of ancient building materials.

CRediT authorship contribution statement

Matteo Maria Niccolò Franceschini: Writing – review & editing, Writing – original draft, Visualization, Investigation, Formal analysis, Data curation. **Emma Cantisani:** Writing – review & editing, Writing – original draft, Visualization, Validation, Supervision, Methodology, Investigation, Formal analysis, Data curation, Conceptualization. **Sara Calandra:** Writing – review & editing, Writing – original draft, Visualization, Validation, Methodology, Investigation, Formal analysis, Data curation. **Giacomo Casa:** Writing – review & editing, Writing – original draft, Visualization, Methodology, Investigation, Data curation. **Mariano Mercurio:** Writing – review & editing, Visualization, Validation, Supervision. **Celestino Grifa:** Writing – review & editing, Visualization, Validation, Supervision, Methodology, Conceptualization. **Gabriel Zuchtriegel:** Writing – review & editing, Validation, Resources. **Valeria Amoretti:** Writing – review & editing, Visualization, Resources. **Tommaso Ismaelli:** Writing – review & editing, Writing – original draft, Visualization, Validation, Supervision, Methodology, Data curation, Conceptualization.

Declaration of Competing Interest

The authors declare that they have no known competing financial interests or personal relationships that could have appeared to influence the work reported in this paper.

Acknowledgments

The authors wish to thank Antonino Russo and Giuseppe Scarpati of the Archaeological Park of Pompei. The activity is supported by the National Recovery and Resilience Plan (NRRP), Project PRRAP019 PE-CHANGES,CUP B53C22003890006, Spoke 8 “Sustainability and Resilience of Tangible Cultural Heritage”, within the research line “Creation of a methodological/operational workflow for ancient built heritage for historical reconstruction, actualisation (restoration - use) and dissemination”.

Appendix A. Supporting information

Supplementary data associated with this article can be found in the online version at doi:10.1016/j.cscm.2024.e03943.

Data Availability

Data will be made available on request.

References

[1] T. Ismaelli, Ancient architectural restoration: approaches and scenarios, in Ancient Architectural Restoration in the Greek World, eds. J. Vanden Broeck-Parant, T. Ismaelli, Proceedings of the international workshop held at Wolfson College (Oxford, February 28 and March 1, 2019), Roma (2021), pp. 19-43.2021.
[2] J.A. Overbeck, A. Mau, Pompeji in seinen Gebäuden, Alterthümern und Kunstwerken, Leipzig, 1884.
[3] A. Mau, Pompeji in Leben und Kunst[2], Leipzig, 1908.
[4] A. Maiuri, L'ultima fase edilizia di Pompei, Roma, 1942.
[5] E. Corti, Ercolano e Pompei. Morte e rinascita di due città, Torino, 1957.
[6] J. Andreau, Histoire des séismes et histoire économique. Le tremblement de terre de Pompéi (62 ap. J.-C.), AnnEconSocCiv 28 (1973) 369–395.
[7] E. La Rocca, A. De Vos, M. De Vos, Pompei[2], Milano, 1976.
[8] J.B. Ward-Perkins, A. Claridge, Pompeii A.D. 79: Treasures from the National Archaeological Museum, Naples, with contributions from the Pompeii Antiquarium and the Museum of Fine Arts, Boston, 1978.
[9] J. Andreau, Il terremoto del 62, in Pompei 79: Raccolta di studi per il decimonono centenario dell'eruzione vesuviana, ed. F. Zevi, Napoli (1979), pp. 40-44.1979.
[10] H. Döhl, P. ZankerLa scultura, in Pompei 79: Raccolta di studi per il decimonono centenario dell'eruzione vesuviana, ed. F. Zevi, Napoli (1979), pp. 177-210. [11] J.B. Ward-Perkins, Roman Imperial Architect1979.
[11] J.B. Ward-Perkins, Roman Imperial Architecture, Harmondsworth, 1981.
[12] A. De Vos, M.De Vos, Pompei, Ercolano, Stabia, Roma, 1982.
[13] J.P. Adam, Observations techniques sur les suites du séisme de 62 à Pompéi", in Tremblements de terre, éruptions volcaniques et vie des hommes dans la Campanie antique (Collection du Centre Jean Bérard 7), ed. C. Albore-Livadie, Napoli, 1986, pp. 67-87.1986.
[14] L. Richardson, Pompeii. An Architectural History, Baltimore-London, 1988.
[15] F.B. Sear, Roman Architecture, London, 1989.
[16] W. Jongman, The Economy and Society of Pompeii, Amsterdam, 1988.
[17] P. Zanker, Pompei. Società, immagini urbane e forme dell'abitare, Torino, 1993.
[18] N. Ruggieri, Seismic protection in Pompeii during the age of Nero and Vespasian, J. Archit. Eng. 23.4 (2017).
[19] N. Ruggieri, Seismic vulnerability of the ancient Pompeii through the evaluation of the 62 AD earthquakes effects, Int. J. Archit. Herit. 11.4 (2017) 490–500.
[20] N. Ruggieri, S. Galassi, G. Tempesta, I terremoti del I secolo d.C. a Pompei. Osservazioni intorno ai danni e consolidamenti nelle Terme Stabiane con particolare riguardo ad uno sperone nel Destrictarium", Restauro Archeol. 26.2 (2018) 72–91.
[21] V. Amato, M. Covolan, H. Dessales, A. Santoriello, Seismic microzonation of the Pompeii Archaeological Park (Southern Italy): local seismic amplification factors, Geosciences 12.275 (2022).
[22] H. Dessales (a cura di), Ricostruire dopo un terremoto. Riparazioni antiche a Pompei, Napoli, 2022.
[23] C. Rispoli, G. Montesano, M. Verde, G. Balassone, S. Columbu, A. De Bonis, C. Di Benedetto, et al., The key to ancient roman mortars hydraulicity: ceramic fragments or volcanic materials? A lesson from the phlegrean Archaeological Area (Southern Italy), Constr. Build. Mater. 411 (2024) 134408, https://doi.org/10.1016/j.conbuildmat.2023.134408.
[24] S. Dilaria, C. Previato, M. Secco, M.S. Busana, J. Bonetto, J. Cappellato, G. Ricci, G. Artioli, P. Tan, Phasing the history of ancient buildings through PCA on mortars' mineralogical profiles: the example of the Sarno Baths (Pompeii), Archaeometry 64 (2022) 866–882.
[25] R. Piovesan, L. Maritan, G. Meneghin, C. Previato, S. Baklouti, R. Sassi, C. Mazzoli, Stones of the façade of the Sarno Baths, Pompeii: a mindful construction choice, J. Cult. Herit. 40 (2019) 255–264.
[26] R. De Luca, D. Miriello, A. Pecci, S. Dominguez-Bella, D. Bernal-Casasola, D. Cottica, A. Bloise, G.M. Crisci, Archaeometric study of mortars from the garum shop at Pompeii, Campania, Italy, Geoarchaeology 30 (2015) 330–335.
[27] M. Secco, C. Previato, A. Addis, G. Zago, A. Kamsteeg, S. Dilaria, C. Canovaro, G. Artioli, J. Bonetto, Mineralogical clustering of the structural mortars from the Sarno Baths, Pompeii: a tool to interpret construction techniques and relative chronologies, J. Cult. Herit. 40 (2019) 265–273.
[28] D. Miriello, A. Bloise, G.M. Crisci, R. De Luca, B. De Nigris, A. Martellone, M. Osanna, R. Pace, A. Pecci, N. Ruggieri, New compositional data on ancient mortars and plasters from Pompeii (Campania – Southern Italy): archaeometric results and considerations about their time evolution, Mater. Charact. 146 (2018) 189–203.
[29] S. Vettori, S. Bracci, E. Cantisani, C. Conti, M. Ricci, Archaeometric and archaeological study of painted plaster from the Church of St. Philip in Hierapolis of Phrygia (Turkey), J. Archaeol. Sci: Rep. 24 (2019) 869–878.
[30] I. Cardoso, M.F. Macedo, F. Vermeulen, C. Corsi, A.Santos Silva, L. Rosado, A. Candeias, J. Mirao, A Multidisciplinary approach to the study of archaeologicalmortars from the Town of Ammaia in the Roman Province of Lusitania (Portugal): archaeological mortars from the Roman town of Ammaia (Lusitania, Portugal), Archaeometry 56 (1) (2014) 1–24.
[31] A. Morricone, A. Macchia, L. Campanella, M. David, S. De Togni, M. Turci, A. Maras, C. Meucci, S. Ronca, Archaeometrical analysis for the characterization of mortars from Ostia Antica, Procedia Chem. 8 (2013) 231–238.
[32] C. Corti, L. Rampazzi, R. Bugini, A. Sansonetti, M. Biraghi, L. Castelletti, I. Nobile, C. Orsenigo, Thermal analysis and archaeological chronology: the ancient mortars of the site of Baradello (Como, Italy), Thermochim. Acta 572 (2013) 71–84.
[33] A. Coutelas, L. Guyard, C.H. David, Pétroarchéologie de mortiers gallo-romains, Application de méthodes analytiques à l'étude des thermes du Vieil-Évreux (Eure), Les nouvelles del'archéologie, 81 (200) 31–36.
[34] L. Bertolini, M. Carsana, M. Gastaldi, F. Lollini, E. Redaelli, Binder of mortars used at different ages in the San Lorenzo church in Milan, Mater. Charact. 80 (2013) 9–20.
[35] I. Ahmad Bany Yaseen, H. Al-Amoush, M. Al-Farajat, A. Mayyas, Petrography and mineralogy of Roman mortars from buildings of the ancient city of Jerash, Jordan, Constr. Build. Mater. 38 (2013) 465–471.
[36] M. Singh, S. Waghmare, S. Vinod, H. Kumar, Characterization of lime plasters used in 16th century Mughal monument, J. Archaeol. Sci. 42 (2014) 430–434.
[37] D. Miriello, L. Barba, J. Blancas, A. Bloise, M. Cappa, M. Cura, D. De Angelis, R. De Luca, A. Pecci, M. Taranto, H.B. Yavuz, G.M. Crisci, New compositional data on ancient mortars from Hagia Sophia (Istanbul, Turkey), Archaeol. Anthropol. Sci. 9 (4) (2017) 499–514.
[38] M. Lezzerini, S. Legnaioli, G. Lorenzetti, V. Palleschi, M. Tamponi, Characterization of historical mortars from the bell tower of St. Nicholas church (Pisa, Italy), Constr. Build. Mater. 69 (2014) 203–212.
[39] M.D. Jackson, S.R. Mulcahy, H. Chen, Y. Li, Q. Li, P. Cappelletti, H.R. Wenk, Phillipsite and Al-tobermorite mineral cements produced through low-temperature water-rock reactions in Roman marine concrete, Am. Mineral. 102 (2017) 1435–1450.
[40] C. Rispoli, S.F. Graziano, C. Di Benedetto, A. De Bonis, V. Guarino, R. Esposito, V. Morra, P. Cappelletti, New insights of historical mortars beyond pompei: the example of Villa del Pezzolo, Sorrento Peninsula, Minerals 9 (2019) 575.
[41] D. Miriello, D. Barca, A. Bloise, A. Ciarallo, G.M. Crisci, F. De Rose, C. Gattuso, F. Gazineo, M.F. La Russa, Characterisation of archaeological mortars from Pompeii (Campania, Italy) and identification of construction phases by compositional data analysis, J. Archaeol. Sci. 37 (2010) 2207–2223.
[42] C. Grifa, S. Barba, F. Fiorillo, C. Germinario, F. Izzo, M. Mercurio, D. Musmeci, et al., The domus of Octavius Quartio in Pompeii: damage diagnosis of the masonries and frescoed surfaces, Int. J. Conserv. Sci. 7 (Spec. Iss. 2) (2016) 885–900.
[43] T. Demauro, Restauri a Pompei (1748-1860), L'Erma di Bretschneider Srl, Roma, 2020.

[44] D. Łatka, P. Matysek, I. Hager, T. Tracz, Assessment of the compressive strength of lime mortar in the joints of brick walls - case study, MATEC Web Conf. 163 (2018) 02006, https://doi.org/10.1051/matecconf/201816302006.
[45] E. Cantisani, S. Calandra, S. Barone, S. Caciagli, M. Fedi, C.A. Garzonio, L. Liccioli, B. Salvadori, T. Salvatici, S. Vettori, The mortars of Giotto's Bell Tower (Florence, Italy): raw materials and technologies, Constr. Build. Mater. 267 (2021) 120801.
[46] C. Grifa, A. De Bonis, A. Langella, M. Mercurio, G. Soricelli, V. Morra, A Late Roman ceramic production from Pompeii, J. Archaeol. Sci. 40 (2) (2013) 810–826.
[47] R. Piovesan, C. Mazzoli, L. Maritan, Production recipes of mortar-based materials from ancient Pompeii by quantitative image analysis approach: the microstratigraphy of plasters in the Temple of Venus, J. Cult. Herit. 59 (2023) 57–68.
[48] F. Izzo, A. Arizzi, P. Cappelletti, G. Cultrone, A. De Bonis, C. Germinario, S.F. Graziano, C. Grifa, V. Guarino, M. Mercurio, V. Morra, A. Langella, The art of building in the Roman period (89 B.C. – 79 A.D.): mortars, plasters and mosaic floors from ancient Stabiae (Naples, Italy), Costr. Build. Mater. 117 (2016) 129–143.
[49] UNI-EN 11176:2006, Cultural heritage. Petrographic description of a mortar, CNR-ICR, Roma, 2006.
[50] J.L. Pouchou, F. Pichoir, Quantitative Analysis of Homogeneous or Stratified Microvolumes Applying the Model "PAP". in: Electron Probe Quantitation, Springer, Boston, MA, USA, 1991, pp. 31–75.
[51] R.S. Boynton. Chemistry and Technology of Lime and Limestone, 2nd ed., John Wiley & Sons, New York, NY, USA, 1980.
[52] A. Bakolas, G. Biscontin, V. Contardi, E. Franceschi, A. Moropoulou, D. Palazzi, E. Zendri, Thermoanalytical research on traditional mortars in Venice, Thermochim. Acta 269/270 (1995) 817–828.
[53] A. Moropoulou, A. Bakolas, K. Bisbikou, Characterization of ancient, byzantine and later historic mortars by thermal and X-ray diffraction techniques, Thermochim. Acta 269–270 (1995) 779–795.
[54] M.P. Riccardi, M. Lezzerini, F. Carò, M. Franzini, B. Messiga, Microtextural and microchemical studies of hydraulic ancient mortars: two analytical approaches to understand pre-industrial technology processes, J. Cult. Herit. 8 (4) (2007) 350–360.
[55] P. Manita, T.C. Triantafillou, Influence of the design materials on the mechanical and physical properties of repair mortars of historic buildings, Mater. Struct. 44 (2011) 1671–1685.
[56] A. Moropoulou, A. Bakolas, P. Moundoulas, E. Aggelakopoulou, S. Anagnostopoulou, Strength development and lime reaction in mortars for repairing historic masonries, Cem. Concr. Compos. 27 (2) (2005) 289–294.
[57] E. Sala, I. Giustina, G.A. Plizzari, Lime mortar with natural pozzolana: historical issues and mechanical behavior. Proceedings of the 6th International Conference on Structural Analysis of Historical Construction, Bath, England, July 2–4 2008, CRC Press, Balkema, London, England, 2008, pp. 957–963.
[58] A. Bakolas, E. Aggelakopoulou, Pozzolanic activity of natural pozzolan-lime pastes and physic mechanical characteristics, J. Therm. Anal. Calorim. 135 (6) (2018) 2953–2961.
[59] M. Monaco, M. Aurilio, A. Tafuro, M. Guadagnuolo, Sustainable mortars for application in the cultural heritage field, Materials 14 (2021) 598, https://doi.org/10.3390/ma14030598.
[60] E. Pecchioni, F. Fratini, E. Cantisani, Atlas of Ancient Mortars in thin section under optical microscope, 2nd ed.; Nardini: Firenze, Italy, 2020; pp. 78.
[61] A. Arizzi, G. Cultrone, Mortars and plasters—how to characterise hydraulic mortars, Archaeol. Anthropol. Sci. 13 (9) (2021) 144.
[62] H.F. Taylor. Cement Chemistry, 2nd ed., Thomas Telford, London, 1997, p. 459.
[63] E.S. Hodgkinson, C.R. Hughes, The mineralogy and geochemistry of cement/rock reactions: high-resolution studies of experimental and analogue materials, Geol. Soc. Lond., Spec. Publ. 157 (1) (1999) 195–211.
[64] Y.E. Qing, Z. Zenan, S. Li, C. Rongshen, A comparative study on the pozzolanic activity between nano-SiO2 and silica fume, J. Wuhan. Univ. Technol. Mater. Sci. Ed. 21 (2006) 153–157.
[65] S. Bruni, F. Cariati, P. Fermo, P. Cairati, G. Alessandrini, L. Toniolo, White lumps in fifth- to seventeenth-century A.D. mortars from Northern Italy, Archaeometry 39 (2007) 1–7.
[66] J.J. Hughes, A.B. Leslie, K. CallebautThe petrography of lime inclusions of historic lime based mortars, in: M. Stamatacis (Ed.), Proceedings of the 8th Euroseminar on Microscopy applied to building materials, Annales Geologiques des pays Helleniques, Athens, 2001, pp. 359-364.2001.
[67] E. Cantisani, F. Fratini, E. Pecchioni, Optical and electronic microscope for mineropetrographic and microchemical studies of lime binders of ancient mortars, Minerals 12 (1) (2022) 41, https://doi.org/10.3390/min12010041.
[68] A.B. Leslie, J.J. Hughes, Binder microstructure in lime mortars: implications for the interpretation of analysis results, Q. J. Eng. Geol. Hydrogeol. 35 (3) (2002) 257–263.
[69] C. Blaeuer, A. Kueng, Examples of microscopic analysis of historic mortars by means of polarising light microscopy of dispersions and thin sections, Mater. Charact. 58 (11-12) (2007) 1199–1207.
[70] S. Pavia, S. Caro, An investigation of Roman mortar technology through the petrographic analysis of archaeological material, Constr. Build. Mater. 22 (8) (2008) 1807–1811.
[71] J. Weber, W. Prochaska, N. Zimmermann, Microscopic techniques to study Roman renders and mural paintings from various sites, Mater. Charact. 60 (7) (2009) 586–593.
[72] G. Bonardi, B. D'Argenio, V. Perrone, Carta geologica dell'Appennino meridionale alla scala 1: 250.000, Mem. della Soc. à Geol. Ital. 41 (1988).
[73] A.K. Chatterjee, Chemico-Mineralogical characteristics of raw materials. in: Advances in Cement Technology, Pergamon, 1983, pp. 39–68.
[74] S.P. Ghosh, Raw Materials - Geological Characteristics. in: Advances in Cement Technology, Pergamon, 1983, pp. 1–37.
[75] M.J.Le Bas, R.W.Le Maitre, A. Streckeisen, B. Zanettin, A chemical classification of volcanic rock based on the total alkali-silica diagram, J. Petrol. 27 (1986) 745–750.
[76] N. Morimoto, J. Fabries, A.K. Ferguson, I.V. Ginzbung, M. Ross, F.A. Seifert, J. Zussman, K. Aoki, G. Gottardi, Nomenclature of pyroxenes, Am. Mineral. 73 (1988) 1123–1133.
[77] J.T. O'Connor, A classification for quartz-rich igneous rock based on feldspar ratios, U. S. Geol. Surv. Prof. Pap. 525B (1965) 79–84.
[78] V. Di Renzo, C. Pelullo, I. Arienzo, L. Civetta, P. Petrosino, M. D'Antonio, Geochemical and Sr-isotopic study of clinopyroxenes from Somma-Vesuvius Lavas: inferences for magmatic processes and eruptive behavior, Minerals 12 (9) (2022) 1114, https://doi.org/10.3390/min12091114.
[79] D. Redi, C. Cannatelli, R. Esposito, A. Lima, P. Petrosino, B. De Vivo, Somma-Vesuvius' activity: a mineral chemistry database, Mineral. Petrol. 111 (1) (2017) 43–67, https://doi.org/10.1007/s00710-016-0462-2.
[80] J.L. Joron, N. Metrich, M. Rosi, R. Santacroce, A. Sbrana, Chemistry and petrography, in: R. Santacrose (Ed.), Monografie finali Somma-Vesuvius, Consiglio Nazionale Delle Ricerche, 1987, pp. 105–174.
[81] V. Morra, D. Calcaterra, P. Cappelletti, A. Colella, L. Fedele, R. De'Gennaro, A. Langella, M. Mercurio, M. De'GennaroDe'Gennaro, Urban geology: Relationships between geological setting and architectural heritage of the Neapolitan area, in M. Beltrando, A. Peccerillo, M. Mattei, S. Conticelli, C. Doglioni, (Eds.), urban geology: Relationships between geological setting and architectural heritage of the Neapolitan area. Journal of the Virtual Explorer, 36 (26) (2010) 1–60.2010.
[82] A. Sbrana, R. Cioni, P. Marianelli, R. Sulpizio, D. Andronico, G. Pasquini, Volcanic evolution of the Somma-Vesuvius Complex (Italy), J. Maps 16 (2) (2020) 137–147.
[83] R. Santacroce, R. Cioni, P. Marianelli, A. Sbrana, R. Sulpizio, G. Zanchetta, D.J. Donahue, J.L. Joron, Age and whole rock–glass compositions of proximal pyroclastics from the major explosive eruptions of Somma-Vesuvius: a review as a tool for distal tephrostratigraphy. J. Volcanol. Geotherm. Res. 177 (2008) 1–18.
[84] M. Barbieri, D. Dolfi, R. Trigila, Sulla genesi dell'analcime delle vulcaniti di Crowsnest alla luce del comportamento geochimico del rubidio nelle blairmoriti e durante il processo di analcimizzazione della leucite fino a P H_2O = 3 Kbar, Rend. Soc. à Ital. Di Mineral. E Petrol. 33 (1) (1977) 55–62.
[85] E. Ruiz-Agudo, C.V. Putnis, J. Hövelmann, P. Á lvarez-Lloret, A. Ibáñez-Velasco, A. Putnis, Experimental study of the replacement of calcite by calcium sulphates, Geochim. Et. Cosmochim. Acta 156 (2015) 75–93.
[86] L. Pastero, R. Giustetto, D. Aquilano, Calcite passivation by gypsum: the role of the cooperative effect, CrystEngComm (2017).

[87] M. Steinby“La produzione laterizia”, in F. Zevi (ed.), Pompei 79: raccolta di studi per il decimonono centenario dell’eruzione vesuviana, Napoli, pp. 265-271.1979.
[88] M. Torelli, Domi nobiles et lateres signati, Actes du Colloque international organisé par le Centre d’histoire urbaine de l’Ecole Normale Supérieure de Fontenay/Saint-Cloud et l’Ecole Française de Rome (Saint-Cloud, 16-18 novembre 1995), Roma, in: P. Boucheron, H. Broise, Y. Thébert (Eds.), La Brique Antiq. Et. M. édiéVal. Prod. Et. Commer. D. ’Un. Mat. ériau (2000) 311–321.
[89] H. Dessales“Les savoir-faire des maçons romains entre connaissance technique et disponibilité des matériaux. Le cas pompéien”, in N. Monteix, N. Tran (éd.), Les savoirs professionnels des gens de métier. Études sur le monde du travail dans le sociétés urbaines de l’empire romain (Collection du Centre Jean Bérard 37), Napoli (2011), pp. 41-63.2011.
[90] M. Covolan, *Tufo gallo: cantieri di costruzione ed economia del tufo a Pompei*, Roma 2023.
[91] H. Dessales, “La produzione laterizia a Pompei: adeguamento di un materiale e organizzazione dei cantieri urbani”, in E. Bukowiecki, R. Volpe, U. Wulf-Rheidt (a cura di), Archeologia dell’Architettura XX. Il laterizio nei cantieri imperiali. Roma e il mediterraneo, Atti del I workshop “Laterizio” (Roma, 27-28 novembre 2014), Firenze (2015), pp. 81-89.2015.
[92] G. Casa, L’altare del Tempio del Genius Augusti. Strategie di restauro e ricostruzione nella Pompei post 62 d.C, *ArchCl* 74 (2023) 741–758.
[93] S. Zanella, Des tas et des remblais. Le remploi des enduits à Pompéi? Un point sur la question (Roma), Remployer Recycl. Restaurer. Les. Autres Vies. Des. enduits Peints (2017) 19–34.